AGU PUBLICATIONS

Tectonics

RESEARCH ARTICLE
10.1002/2015TC004040

Key Points:
- Radioactive decay was the primary cause of ultrahigh-temperature metamorphism
- A zone of concentrated heat-producing elements caused focused heating
- Monazite stability enabled the retention of heat-producing elements in the middle crust

Supporting Information:
- Texts S1 and S2 and Tables S1–S4

Correspondence to:
F. Horton,
horton@caltech.edu

Citation:
Horton, F., B. Hacker, A. Kylander-Clark, R. Holder, and N. Jöns (2016), Focused radiogenic heating of middle crust caused ultrahigh temperatures in southern Madagascar, *Tectonics*, *35*, doi:10.1002/2015TC004040.

Received 24 SEP 2015
Accepted 7 JAN 2016
Accepted article online 12 JAN 2016

Focused radiogenic heating of middle crust caused ultrahigh temperatures in southern Madagascar

Forrest Horton[1,2], Bradley Hacker[1], Andrew Kylander-Clark[1], Robert Holder[1], and Niels Jöns[3]

[1]Department of Earth Science, University of California, Santa Barbara, California, USA, [2]Now at California Institute of Technology, Pasadena, California, USA, [3]Department of Geology, Mineralogy and Geophysics, Ruhr University Bochum, Bochum, Germany

Abstract Internal heating can cause melting, metamorphism, and crustal weakening in convergent orogens. This study evaluates the role of radiogenic heat production (RHP) in a Neoproterozoic ultrahigh-temperature metamorphic (UHTM) terrane exposed in southern Madagascar. Monazite and zircon geochronology indicates that the Paleoproterozoic Androyen and Anosyen domains (i) collided with the oceanic Vohibory Arc at ~630 Ma, (ii) became incorporated into the Gondwanan collisional orogen by ~580 Ma, and (iii) were exhumed during crustal thinning at 525–510 Ma. Ti-in-quartz and Zr-in-rutile thermometry reveals that UHTM occurred over >20,000 km^2, mostly within the Anosyen domain. Assuming that U, Th, and K contents of samples from the field area are representative of the middle to lower crust during orogenesis, RHP was high enough—locally >5 μW/m^3—to cause regional UHTM in <60 Myr. We conclude that, due in large part to the stability and insolubility of monazite at high crustal temperatures, RHP was the principal heat source responsible for UHTM, obviating the need to evoke external heat sources. Focused RHP probably thermally weakened portions of the middle crust, gravitationally destabilizing the orogen and facilitating thinning via lateral extrusion of hot crustal sections.

1. Introduction

As zones of focused metamorphism, melting, and ductile deformation, hot crustal sections are especially important for understanding the evolution of the middle and lower crust in convergent orogens. Extreme regional metamorphism at ≥900°C is referred to as ultrahigh-temperature metamorphism (UHTM). Such temperatures are increasingly recognized in continental collision zones worldwide [*Kelsey*, 2008; *Kelsey and Hand*, 2014, and references therein], and geophysical evidence [*Mechie et al*., 2004; *Unsworth et al*., 2005] and granulite xenoliths [*Hacker et al*., 2000] suggest that UHTM is occurring beneath the Tibetan plateau. In many UHT orogens, the extreme temperatures appear to have been sustained for >40 Myr [*Kelsey and Hand*, 2014], despite the fact that prograde [e.g., *Lyubetskaya and Ague*, 2009] and melting reactions [e.g., *Thompson and Connolly*, 1995] are endothermic and buffer temperature increases.

Ultrahigh temperatures in continental crust that exceed the conductive geotherm require heat advection and/or heat production, yet such heating mechanisms remain difficult to detect and are poorly quantified. Heat from the mantle can advect in several ways. For example, high seismic wave speeds at the base of continental crust have been interpreted as underplated basalt [e.g., *Rudnick and Jackson*, 1995], which can cause melting [*Dufek and Bergantz*, 2005] and UHTM [*Annen et al*., 2006; *Dewey et al*., 2006] in the lowermost crust. Alternatively, amagmatic mantle heat advection can occur in subduction-to-collision orogens when hot back arcs contract [*Currie and Hyndman*, 2006; *Brown*, 2008].

Endogenous continental heat can be produced by mechanical heating and radioactive decay. Mechanical heating (also referred to as shear heating or viscous dissipation) of strong rocks in continental collision zones may be significant [e.g., *Kincaid and Silver*, 1996; *Stüwe*, 1998; *Burg and Gerya*, 2005], especially in shear zones [*Nabelek et al*., 2010]. However, mechanical heat production is probably most effective below 600°C due to the negative feedback between mechanical heating and thermal weakening [*Stüwe*, 2007]. The natural abundances of the dominant heat-producing elements (HPEs) U, Th, and K are variable and strongly influence crustal temperature and therefore rheology [e.g., *England and Thompson*, 1984; *Le Pichon et al*., 1997]. Given sufficient time and thickened crust, radiogenic heat production (RHP) can lead to UHTM [*McKenzie and Priestley*, 2008; *Clark et al*., 2011, 2014]. Because HPEs are generally incompatible during melting of the crust and mantle, magmatic processes are thought to concentrate HPEs in the upper continental crust [*Bea*, 2012]. Despite this, the vertical distribution of HPEs in deep boreholes and exposed crustal sections does not correlate with depth [e.g., *Furlong and Chapman*, 2013], and some deep crustal granulites contain abundant U, Th, and K [*Behn et al*., 2011]. Recent evaluations of seismic wave speed and heat flow data have even suggested that the lower crust could be quite radiogenic [*Hacker et al*., 2011, 2015]. But the role of RHP remains controversial because heat-production rates for the middle and lower crust are difficult to quantify [*Jaupart and Mareschal*, 2003; *Hacker et al*., 2011, 2015] and because the removal of HPEs during the migration of melts may limit the importance of RHP at hypersolidus temperatures [e.g., *Sandiford and McLaren*, 2002; *Bea*, 2012].

The objective of this study is to evaluate the role of RHP in contractional tectonic settings—and with respect to UHTM, in particular—by studying the Neoproterozoic-Cambrian continent-continent collision zone exposed in southern Madagascar. First, we evaluate and supplement the previous U/Th-Pb geochronology across southern Madagascar to assess the duration of orogenesis and high temperatures. Second, we apply 4+ cation thermometry to constrain peak temperatures and isotherms geographically. Third, we employ two-dimensional numerical modeling based on (i) geochronology, (ii) thermometry, and (iii) whole-rock compositions across southern Madagascar to appraise heterogeneous crustal heat production during orogenesis. This modeling approach differs from other studies [e.g., *England and Thompson*, 1984; *Beaumont et al*., 2004, 2010; *Jamieson et al*., 2004, 2006; *Sizova et al*., 2014] by calculating spatially varying heat production from U, Th, and K concentrations in rocks rather than assuming a uniform lateral distribution; our results highlight some of the problems associated with such assumptions. After assessing the effects of RHP during the assembly of Gondwana, we address broader questions that apply to orogens worldwide: Why do some metamorphic protoliths contain especially high concentrations of HPEs? How mobile are HPEs during metamorphism and melting? And to what extent can RHP cause thermal anomalies in thickened crust?

2. Geologic Background

Southern Madagascar exposes a lower crustal section of the collisional orogen that formed during the late Neoproterozoic–Early Cambrian collision of East and West Gondwana [*Stern*, 1994; *Collins and Pisarevsky*, 2005; *Tucker et al*., 2014]. It is presumed to be analogous to the present-day India-Eurasia collision because it extends over a large region from the Middle East through East Africa, Madagascar, Southern India, Sri Lanka, and Antarctica [*Collins and Windley*, 2002].

Extensive metamorphism, melting, and ductile shearing during the assembly of Gondwana obfuscated the precollision geologic record in Madagascar such that the ages of protoliths and locations of major sutures remain uncertain. Prior to collision, the Archean Dharwar and Congo/Tanzania cratons of East and West Gondwana, respectively, were separated by the Neoarchean-Paleoproterozoic Antananarivo domain. The Antananarivo domain was either the western margin of East Gondwana [*Muller*, 2000; *GAF-BGR*, 2008 (GAF-BGR is sponsored by the *Projet de Gouvernance des Ressources Minerales, Madagascar* (a program funded by the World Bank), an international consortium of scientists conducted four years of research across Madagascar, the results of which were compiled into a final report by the German firms GAF-AG and BGR, and then published by Madagascar's Ministry of Energy and Mines in 2008.); *Tucker et al*., 2011, 2014; *Ichiki et al*., 2015] or part of a microcontinent (Azania) that collided first with West Gondwana and later with East Gondwana [*Collins and Pisarevsky*, 2005; *Collins et al*., 2014]. Prior to the final assembly of Gondwana, much of central Madagascar, including the Antananarivo domain, was intruded by the ~850–700 Ma Imorona-Itsindro suite that has been attributed to either intracontinental extension [*Tucker et al*., 2011, 2014], a west facing continental magmatic arc on the western margin of East Gondwana [*Muller*, 2000; *GAF-BGR*, 2008; *Moine et al*., 2014; *Ichiki et al*., 2015], or an east facing continental arc on the eastern margin of Azania [*Collins and Pisarevsky*, 2005]; these plutonic rocks are notably absent in southern Madagascar. During continent-continent collision, Mesoproterozoic and Neoproterozoic sedimentary rocks deposited on the Archean and Paleoproterozoic crust became folded into and intercalated with the older crust [*Tucker et al*., 2014].

Tectonic domains in southern Madagascar (Figure 1) are delineated by major ductile shear zones [e.g., *Windley et al*., 1994]. The Vohibory, Androyen, and Anosyen domains are separated by the Ampanihy and Beraketa shear zones, respectively [*de Wit et al*., 2001; *Tucker et al*., 2011]. The westernmost Vohibory domain is a mélange of ultramafic and felsic volcanic rock, terrigenous sedimentary rock, and chemical sedimentary rock [*de Wit*, 2003; *Collins*, 2006; *GAF-BGR*, 2008] that formed as part of an intraoceanic arc at 670–630 Ma before becoming involved in the East-West Gondwana collision [*Jöns and Schenk*, 2008].

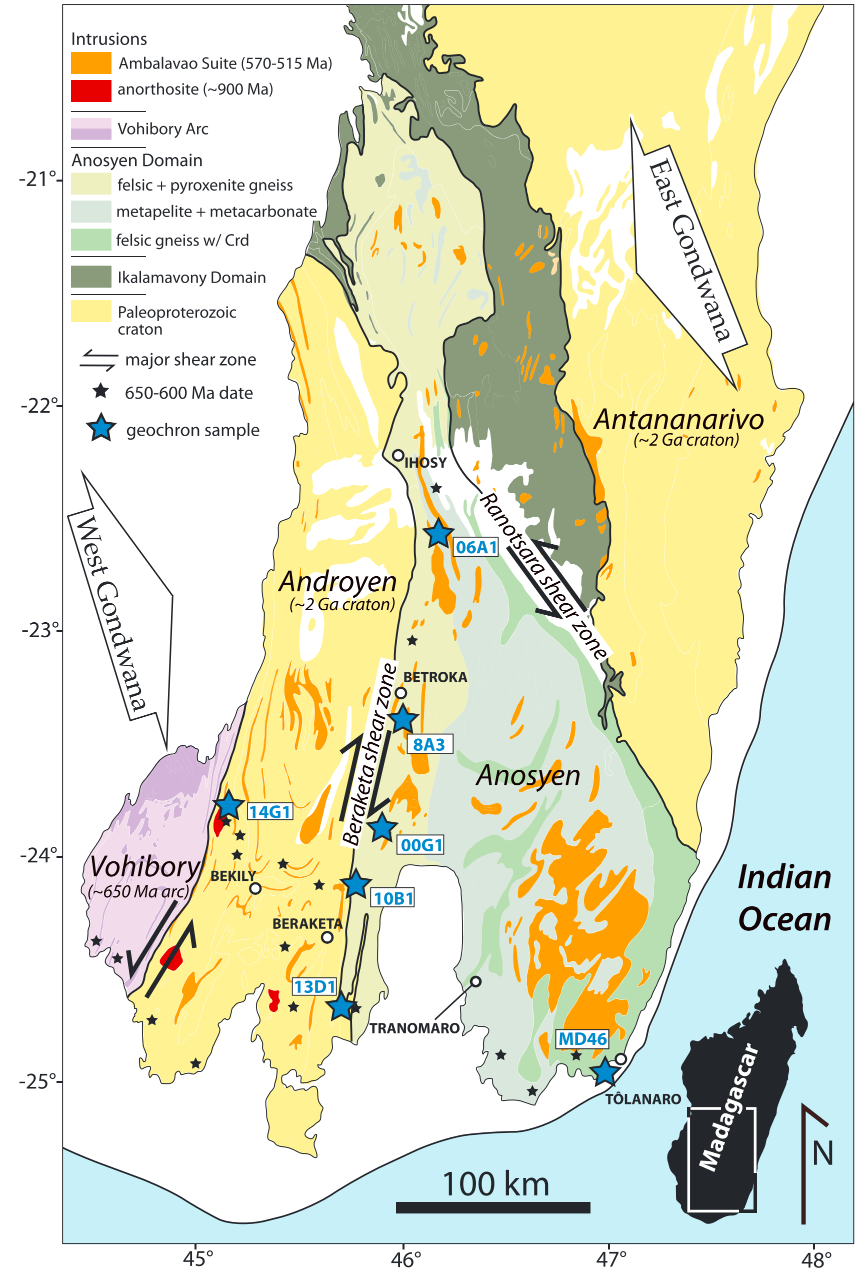

Figure 1. Lithotectonic map of southern Madagascar based on *GAF-BGR* [2008] showing geochronology sample locations.

Immediately to the east, the Androyen domain consists of paragneisses and felsic metavolcanic rocks, the protoliths of which are probably Paleoproterozoic [*Tucker et al.*, 2014] and certainly predate the intrusion of ~900 Ma anorthosites [*GAF-BGR*, 2008]. The Anosyen domain contains aluminous metasediments, calcsilicates, and interbedded quartzofeldspathic volcanosedimentary rocks [*Kröner et al.*, 1996, 1999; *Muller*, 2000; *GAF-BGR*, 2008] that are genetically related to the Imorona-Itsindro suite [*GAF-BGR*, 2008], as well as older, Paleoproterozoic crust [*Tucker et al.*, 2011, 2014, and references therein]. Separating the southern Madagascar domains from the Antananarivo domain in the northeast is the Ranotsara shear zone and Ikalamavony domain, which have a lower portion with Archean-Paleoproterozoic detrital zircons and an upper portion with ~1 Ga arc-related metavolcanic and metasedimentary rocks [*Handke et al.*, 1999; *Handke*, 2001; *Tucker et al.*, 2007, 2011]. The metapelites and calcsilicates of the Anosyen domain may have been deposited as a marginal sequence on West Gondwana [*Muller*, 2000], Azania [*Collins and Pisarevsky*, 2005] or East Gondwana [*GAF-BGR*, 2008], or in an intracontinental basin [*Tucker et al.*, 2014]. Accordingly, the suture between East and West Gondwana may be along the east or west edges of the Antananarivo domain [*Collins and Pisarevsky*, 2005], the Ranotsara shear zone [*Muller*, 2000], the Beraketa shear zone [*GAF-BGR*, 2008; *Boger et al*., 2014], or west of the Androyen domain [*Tucker et al*., 2014]. The position of the Anosyen domain during orogenesis, however, is undisputed: initially deposited on top of older crust, the Anosyen rocks became sandwiched between (yet probably remained underlain by) older Paleoproterozoic terranes.

The earliest metamorphism associated with Gondwana assembly in southern Madagascar occurred at 630–600 Ma and is almost exclusively observed west of the Beraketa shear zone in the Vohibory and Androyen domains [*GAF-BGR*, 2008]; this event may represent the accretion of the Vohibory Arc to either Azania [*Jöns and Schenk*, 2008], an exotic Androyen microcontinent of East African affinity [*GAF-BGR*, 2008], or the western margin of East Gondwana [*Tucker et al*., 2014] prior to closure of the Mozambique Ocean. Peak conditions associated with this event were initially estimated to be ~800–850°C at 9–12 kbar [*Nicollet*, 1989; *Martelat et al*., 1997; *Jöns and Schenk*, 2008] but may be lower (750–800°C at 7–8 kbar) [*GAF-BGR*, 2008]. The main stage of orogenesis that affected all of central and southern Madagascar occurred at ~585–520 Ma [*Berger et al*., 2006; *GAF-BGR*, 2008; *Giese et al*., 2011]. UHT mineral assemblages (orthopyroxene + sillimanite + quartz, osumilite + garnet), Al-in-orthopyroxene thermometry, and pseudosections record the highest peak conditions of $>$900°C at 9–10 kbar [*GAF-BGR*, 2008; *Jöns and Schenk*, 2011] or 880–920°C at 6–6.5 kbar [*Boger et al*., 2012] in the southern Anosyen domain; osumilite growth in this region [*Jöns and Schenk*, 2011] probably occurred at pressures $<$8.5 kbar [*Harley*, 2008; *Kelsey*, 2008]. Peak conditions in the northern Anosyen domain were probably 50–100°C and 1 kbar lower. Modestly lower peak conditions of ~850°C at 6.5–8 kbar were also reached in the Androyen domain [*Martelat et al*., 1997; *Markl et al*., 2000; *GAF-BGR*, 2008]. In the Ikalamavony domain, which was translated east over the Antananarivo domain as a fold-thrust belt during orogenesis, temperatures peaked at ~700°C [*GAF-BGR*, 2008]. Predeformation to syndeformation granites, the Ambalavao suite, intruded the Anosyen and Androyen domains from ~580 to 565 Ma and postdeformation granitic plutonism—presumably corresponding to the rapid exhumation of the Anosyen domain from 35 km to 10–20 km depth—occurred throughout south and central Madagascar from ~530 to 510 Ma [*GAF-BGR*, 2008].

The Vohibory, Androyen, and Anosyen domains have strong polyphase, granulite-facies fabrics. Early structures include ENE-WSW trending stretching lineations and fold axes [*Paquette et al*., 1994; *de Wit et al*., 2001]. Large-scale remote sensing and outcrop-scale fabrics show that the intensity of this strain increases westward [*Martelat et al*., 2000]. In the west, some or most of these fabrics may have formed when the Androyen domain was thrust beneath the Vohibory domain [*de Wit et al*., 2001]. In the Anosyen domain, however, early structures are ascribed to crustal thickening from 580 to 565 Ma [*Nédélec et al*., 1995; *Paquette et al*., 1994]. A younger series of subvertical, ductile strike-slip shear zones (5–20 km wide) separate the intervening lower strain domains [*Windley et al*., 1994]; if shear along these zones was coeval with E-W shortening and N-S stretching, the overall deformation may have produced crustal thinning and the southward extrusion of the southern Anosyen domain relative to the Antananarivo domain [*Martelat et al*., 2000; *Schreurs et al*., 2010]. North of Ihosy, the Anosyen domain is highly strained, isoclinally folded, and forms a flower-like shape, suggesting that ductile flow of the Anosyen domain under granulite-facies conditions led to northward tectonic extrusion [*Tucker et al*., 2014]. Thus, the Antananarivo domain probably acted as a rigid indenter, extruding the semirigid southern Anosyen domain southward and the ductile northern Anosyen domain northward.

3. Geochronology

The accumulation of significant radiogenic heat requires a heat source of sufficient power and size that operates long enough in a material of low thermal diffusivity. Evaluating this in nature requires determining the 3-D distribution and abundances of HPEs, the evolution of crustal thickness, and the timescales of metamorphism. Below, we discuss previously published geochronology of Madagascar pertaining to the collision of East and West Gondwana and then present new U/Th-Pb geochronology that provides additional constraints.

3.1. Previous Geochronology

Igneous zircon dates from rocks interlayered with Vohibory basalts suggest that most of the Vohibory domain grew between 670 and 630 Ma [*GAF-BGR*, 2008; *Tucker et al*., 2014]. Rb-Sr whole rock [*Windley et al*., 1994] and U-Pb/Pb-Pb magmatic zircon core dates [*Emmel et al*., 2008; *Jöns and Schenk*, 2008] suggest that parts of the Vohibory domain may be as old as 850–700 Ma, but these older ages may be from a window into the Androyen domain. The earliest metamorphic dates in the southwestern Androyen domain suggest that accretion of the Vohibory Arc to the Androyen domain may have occurred as early as 650–640 Ma [*de Wit et al.*, 2001; *Emmel et al.*, 2008; *Jöns and Schenk*, 2011], but metamorphism associated with the accretion continued through ~630–600 Ma [*GAF-BGR*, 2008; *Jöns and Schenk*, 2008]. Arc-type magmatism may have continued during orogenesis because calc-alkaline igneous rocks were emplaced until ~610 Ma [*Tucker et al.*, 2014]. Although ubiquitous throughout the Androyen domain [*Paquette and Nédélec*, 1998; *de Wit et al.*, 2001; *GAF-BGR*, 2008; *Jöns and Schenk*, 2011; *Boger et al.*, 2014], metamorphic zircon and monazite U-Pb dates of 630–610 Ma have not been observed in the Anosyen domain farther east [*GAF-BGR*, 2008].

The main stage of orogenesis in southern Madagascar [*GAF-BGR*, 2008] is bracketed by early syndeformation plutons (576 ± 4 Ma in the Androyen domain and 573 ± 6 Ma in the Anosyen domain) and late deformation to postdeformation plutons (541 ± 2 Ma in the Androyen domain and 521 ± 12 Ma in the Anosyen domain) of the Ambalavao suite. Metamorphic dates reported across both domains largely fall in the same interval [*Paquette et al.*, 1994; *Kröner et al.*, 1999; *Martelat et al.*, 2000; *Muller*, 2000; *de Wit et al.*, 2001; *GAF-BGR*, 2008; *Collins et al.*, 2012; *Giese et al.*, 2011; *Tucker et al.*, 2011; *Boger et al.*, 2014]. The preponderance of igneous and metamorphic dates across southern Madagascar during this interval (Figure 3) is highlighted in the detailed synopsis provided by *Tucker et al.* [2014]; metamorphism in the Antananarivo domain to the east probably initiated later [*Tucker et al.*, 2014] and persisted longer (until nearly 500 Ma) [*Giese et al.*, 2011]. The main stage of Gondwana assembly was complete by ~520 Ma, when the nondeformed Ambalavao granites were intruded across the region and after which metamorphic dates in the Androyen and Anosyen domains are no longer observed. Dates <500 Ma obtained in major shear zones may reflect late fluid circulation [*Martelat et al.*, 2000].

3.2. When Were Southern Madagascar Domains Buried?

Two end-member scenarios emerge from previous southern Madagascar geochronology:

1. The accretion of the Vohibory arc may have been a tectonometamorphic event distinct from the main stage of orogenesis, affecting exclusively the Vohibory and Androyen domains and ending >20 Myr prior to the main stage of orogeny. If so, thickened crust during the Gondwanan collisional orogenesis may have existed for ~60 Myr (580–520 Ma).
2. Alternatively, tectonic burial, crustal thickening, and high-temperature metamorphism affected all of southern Madagascar shortly after the accretion of the Vohibory arc (~630 Ma) and persisted until ~520 Ma, when postdeformation granites signal the cessation of orogenesis. In this case, thickened crust may have persisted for >100 Myr and the dearth of 630–610 Ma metamorphic dates in the Anosyen domain [*GAF-BGR*, 2008] could be explained by overprinting during subsequent higher-temperature metamorphism.

To distinguish between these scenarios, in situ laser-ablation split-stream (LASS) inductively coupled plasma-mass spectrometry (ICP-MS) U/Th-Pb geochronology and trace element geochemistry analyses were conducted on monazites and zircons from across the Androyen and Anosyen domains (see Text S1 in the supporting information for LASS methods and Table S4 for analytical data). Most zircons in the metamorphic rocks are small (<50 μm), euhedral, have oscillatory zoning, and yielded late Neoproterozoic U-Pb dates (few inherited zircons have been found); this suggests that if zircon existed in the protolith, much of it (a) recrystallized or (b) dissolved into melt or rutile during peak metamorphism and reprecipitated during cooling. In contrast, monazites tend to be large (>100 μm) and preserve an inherited component and a wider range of metamorphic dates. For example, a garnet-cordierite gneiss (sample 06C1) contains large metamorphic Paleoproterozoic monazites (>1 mm) in which the U-Pb system was largely reset during the assembly of Gondwana (Figure 2).

Two samples (see Text S2 and Table S3 for petrographic descriptions and mineral assemblages, respectively) in the Androyen domain have monazite dates >600 Ma. A metapelite with euhedral garnet porphyroblasts (sample 14G1) from immediately west of the Ankafotra anorthosite body near the Androyen-Vohibory contact has concordant monazite dates that range from 614 ± 17 Ma to ~522 Ma (Figure 2). Discordant dates dispersed toward 2.2 Ga (not shown in figure) indicate that the highest-Y portion of the mottled monazite cores are relict Paleoproterozoic material. The cores probably underwent dissolution/reprecipitation or in situ recrystallization beginning at ~614 Ma, and low-Y metamorphic rims grew from ~550 to 522 Ma. All spot analyses have negative Eu anomalies, but spot dates <580 Ma have more pronounced Eu anomalies. The Lu/Dy ratio decreased at ~600 Ma and remained low, with the exception of the two youngest analyses at ~522 Ma; low Lu/Dy during this interval may be indicative of monazite (re)crystallization in the presence of garnet. A migmatitic gneiss (sample 13D1) from the southernmost Beraketa shear zone that contains sillimanite in

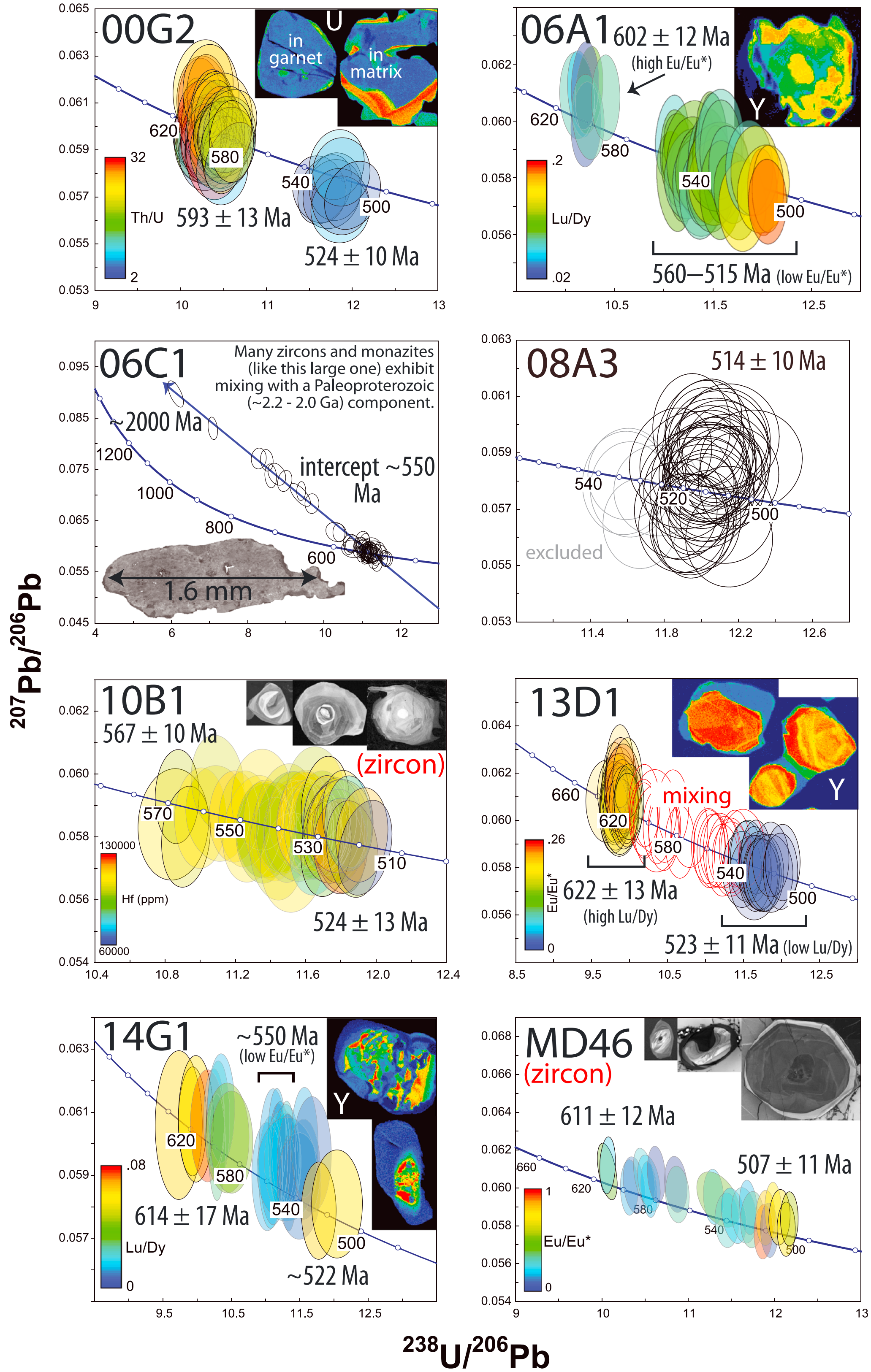

Figure 2. Concordia diagrams for LASS results. Error ellipses are 2σ are colored by trace element concentration in some cases. Ages and uncertainty for clusters of data points (bold ellipses) with MSWD < 1 and are reported in mega annum. Red ellipses are suspected to be mixed ages. Zircon cathodoluminescence images are shown for samples 10B1 and MD46; all other grain maps were made on the electron microprobe.

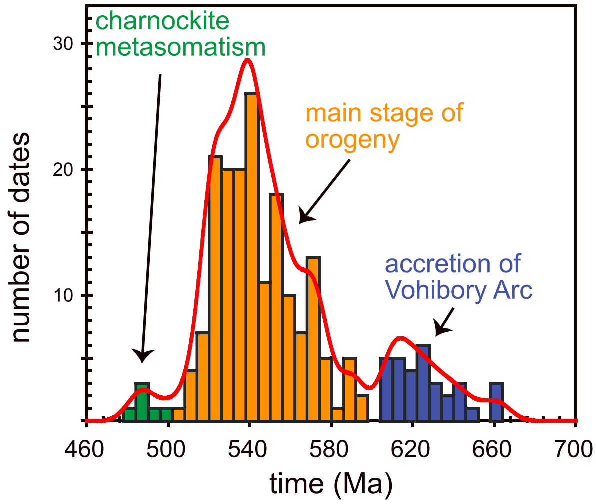

Figure 3. Probability density distribution for geochonologic dates from across Madagascar (based on the data compilation in *Tucker et al.* [2014]).

and around garnet porphyroblasts yields a comparable range of monazite dates from 622 ± 13 Ma to 523 ± 11 Ma without any inheritance (Figure 2). Oscillatory zoning of the high-Y monazite cores is cut by dissolution embayments and overgrown by low-Y metamorphic rims; the sharply delineated cores and rims suggest that the analyses that yield intermediate dates are mixtures of core and rim material. The older population has less-pronounced Eu anomalies and higher Lu/Dy.

Several samples in the Anosyen domain also yielded ~600 Ma dates. Monazites in a cordierite–sillimanite gneiss collected south of Ihosy (sample 06A1) have relic high-Y Paleoproterozoic cores. These monazites retain 602 ± 12 Ma dates and a range of younger dates from ~560 Ma to 515 Ma that have more pronounced Eu anomalies (Figure 2). Lu/Dy is anticorrelated with age. Farther south along the Beraketa shear zone, a gneissic sample (sample 00G2) contains sapphirine and large garnet porphyroblasts with cordierite symplectite overgrown by orthopyroxene-spinel symplectite. Monazites shielded in garnet have relatively homogenous trace element compositions, whereas monazites in the matrix have irregularly shaped cores with uranium-rich embayments consistent with dissolution. The cores have a weighted mean date of 593 ± 13 Ma (MSWD = 0.98, n = 44), and the rims give a date of 524 ± 10 (MSWD = 0.73, n = 9). This range is also recorded by zircon in a garnet-orthopyroxene gneiss from the south central Anosyen domain (sample MD46): discordant dates scatter toward ~2.2 Ga, but concordant metamorphic dates range from ~611 Ma to ~507 Ma with increasingly pronounced Eu anomalies (Figure 2).

3.3. Did Accretion of the Vohibory Arc Produce Thickening and Accretion Farther East?

The distinct trace element signature of the >600 Ma monazite domains—high Lu/Dy, high-Y cores, and less-pronounced Eu anomalies—in samples from either edge of the Androyen domain (13D1 and 14G1) may suggest that an early metamorphism occurred when garnet was scarce or absent [e.g., *Zhu and O'nions*, 1999; *Foster et al.*, 2000, 2002; *Rubatto et al.*, 2013; *Stearns et al.*, 2013]. Contrary to earlier reports [*GAF-BGR*, 2008], we observe this early metamorphic record in the Anosyen domain as well, revealing that this early event affected a broader area than previously recognized and implying that the Anosyen and Androyen domains may have been joined prior to 600 Ma. Although accretion of the Vohibory arc may have initiated as early as ~650 Ma, metamorphism related to this collision occurred from ~620 to 600 Ma and had propagated eastward at least as far as the Anosyen domain by this time; it remains unclear whether heat inherited from the arc system and/or crustal thickening caused metamorphism. There are relatively few published dates in the 600–580 Ma range (Figure 3) [*Tucker et al.*, 2014], suggesting a period of tectonic quiescence. If monazite in 06A1 and 14G1 grew in response to tectonic burial, our data suggest that parts of the Androyen and Anosyen domains were incorporated into a thickened crustal pile prior to the main stage of orogenesis that began at ~580 Ma. If so, the accretion of the Vohibory arc—although a temporally distinct tectonometamorphic event—may have been an important prelude to subsequent orogenesis, insulating heat-producing crust at depth prior to continent-continent collision.

3.4. When Were Southern Madagascar Domains Exhumed?

The prevalence of 540–520 Ma dates across Madagascar reflects accessory phase growth during late orogenic cooling and granite emplacement (Figure 3). The end of orogenesis likely coincided with the youngest metamorphic dates and the emplacement of nondeformed Ambalavao granites. Oscillatory-zoned, CL-dark zircons from a garnet-cordierite-orthopyroxene gneiss (sample 10B1) collected within the southern Beraketa shear zone yield a range of dates from 567 ± 10 Ma to 524 ± 13 Ma (Figure 2). These zircons have oscillatory zoning consistent with crystallization from partial melt. Also within the Beraketa shear zone, monazites from a meter-scale pod (sample 08A3) of coarse cordierite with spinel and corundum—presumably formed by fluid infiltration of the shear zone during the waning stages of metamorphism—have a weighted mean age of 514 ± 10 Ma (MSWD = 0.83, n = 43). Collectively, the youngest metamorphic spot dates we obtained in southern Madagascar (from samples 00G2, 06A1, 10B1, 13D1, 14G1, and MD46) range from 525 to 507 Ma.

Younger dates obtained in the region are likely due to fluid circulation in shear zones in the brittle upper crust at <500 Ma [e.g., *Martelat et al*., 2000]. Phlogopite deposits in the Beraketa shear zone have yielded calcite-phlogopite two-point Rb-Sr isochrons of 491 ± 10 and 492 ± 10 Ma [*Martin et al*., 2013] and K-Ar ages of 491–485 Ma [*Rakotondrazafy et al*., 1997] and a single Ar-Ar date of 481 ± 2 Ma [*Martin et al*., 2013]. A zircon-bearing calcite vein in the southern Anosyen domain has a zircon U-Pb date of 523 ± 5 Ma [*Paquette et al*., 1994]. In southern India—adjacent to southern Madagascar at the time—520–510 Ma zircon rims [*Whitehouse et al*., 2014] and 495 Ma monazite domains [*Taylor et al*., 2014] have been linked to fluid-induced dehydration reactions (i.e., charnockitization); we interpret the coeval dates reported in southern Madagascar to this regional metasomatic event that postdates orogenesis by up to 20 Myr.

Given these constraints, the Vohibory Arc probably accreted at ~645 [*de Wit et al*., 2001] or 620 Ma [*GAF-BGR*, 2008] causing metamorphism of the Androyen domain and at least part of the Anosyen domain from ~620–600 Ma. Heat from the arc could explain regional metamorphism at low to moderate pressure [e.g., *GAF-BGR*, 2008] and minimal crustal thickening. Alternatively, metamorphism could have occurred in response to burial to greater depth [e.g., *Nicollet*, 1990; *Martelat et al*., 1997; *Jöns and Schenk*, 2008], in which case, thickening of the continental margin could have persisted for 40–65 Myr prior to the collision of East and West Gondwana. The formation of a broad orogenic plateau likely occurred during the main stage of orogenesis that began at ~580 Ma and lasted for ~65 Myr.

4. Thermometry

The degree of crustal heating can be broadly constrained by the areal extent of peak metamorphic isotherms. The following section summarizes previous thermal constraints based on mineral assemblages [*Jöns and Schenk*, 2011] and phase diagrams [*GAF-BGR*, 2008] and then presents new 4+ cation thermometry.

4.1. Previous Thermal Constraints

Mineral assemblages reported by *Jöns and Schenk* [2011] provide a first-order measure of the area affected by UHTM (Figure 5). The UHTM diagnostic [e.g., *Harley*, 2008] assemblage garnet + osumilite (inferred from pseudomorphs containing cordierite + K-feldspar + orthopyroxene or cordierite + K-feldspar + quartz + biotite) is observed in the southern Anosyen domain west of Tôlanaro and north of Tranomaro. Osumilite pseudomorphs in garnet-absent rocks are also found near Tranomaro; although not diagnostic, these are probable indicators of UHTM. Sapphirine + quartz and Al-rich orthopyroxene + sillimanite + quartz assemblages—also likely indicators of UHTM but stable to lower temperatures under oxidizing conditions [*Harley*, 2008]—exist along the southernmost Beraketa shear zone. Spinel + quartz assemblages are found across a much larger area from Tôlanaro to Bekily in the west and Ihosy in the north. Spinel + quartz is not diagnostic of UHTM, but probably still indicative of temperatures >800°C [*Harley*, 2008, and references therein]. The absence of UHTM assemblages in the central and northern Anosyen domain represents a northward decreasing metamorphic grade, and the lack of UHTM and spinel + quartz assemblages in the western part of the Androyen domain indicates lower peak temperatures to the west [*Jöns and Schenk*, 2011].

GAF-BGR [2008] constructed two phase diagrams using the NCKFMASHTO model system intended to be representative of Anosyen domain rocks. Most indicative of UHTM are the gneissic bands of cordierite-rich (cordierite was presumed to be retrograde), spinel- and magnetite-bearing Bakika formation that are only exposed in the southeastern Anosyen domain: the peak assemblage of garnet ± orthopyroxene + magnetite + ilmenite + spinel + two feldspars + quartz constrains temperatures to >880°C. The Bakika formation contains a significant fraction of ferric iron. The regionally extensive cordierite- and magnetite-rich Ihosy formation is also highly oxidized and has a similar composition, so the occurrence of orthopyroxene and garnet in the Ihosy gneisses also indicates that temperatures locally exceeded >880°C. Elsewhere in the Ihosy formation, the absence of garnet and orthopyroxene indicates slightly lower temperatures of ~870°C. In contrast, the garnet + biotite + sillimanite + ilmenite + spinel

Table 1. Summary of 4+ Cation Thermometry Results[a]

Sample ID	Latitude (° WGS84)	Longitude (° WGS84)	Number of Grains	Number of Analyses	Mean Ti (ppm)	Maximum Ti (ppm)	Mean Temp. (°C)	Maximum Temp. (°C)
				Ti-in-Quartz (EPMA) After Thomas et al. [2010]				
00G2	−23.812599	45.814301	4	32	184	265	827	878
03 F1	−22.508819	45.556252	6	33	61	109	696	765
10B1	−24.073637	45.690013	10	69	214	327	845	908
11C1	−25.022338	46.647301	5	32	242	336	864	912
11E1	−24.793386	46.864845	3	53	208	259	844	875
13D1	−24.656649	45.556724	9	36	118	176	772	823
MD46	−25.02237778	46.64708056	6	189	288	388	888	934
MD62	−24.72223611	46.43896667	4	76	207	301	838	896
MD81	−24.33060556	45.83311667	4	82	170	241	816	865
MD84	−24.45060556	45.80064167	4	52	198	225	838	855
				Ti-in-Quartz (ICP-MS) After Thomas et al. [2010]				
10B1	−24.073637	45.690013	1	24	300	372	894	927
MD46	−25.02237778	46.64708056	1	11	338	389	912	934
MD54	−25.00815833	46.97716667	1	11	372	441	926	954
MD90	−24.107025	45.694725	4	28	232	339	856	913
				Zr-in-Rutile (EPMA) After Ferry and Watson [2007]				
10B1	−24.073637	45.690013	8	139	2496	4499	836	930
MD90	−24.107025	45.694725	6	170	3559	5848	896	967

[a]See Table S5 for complete results.

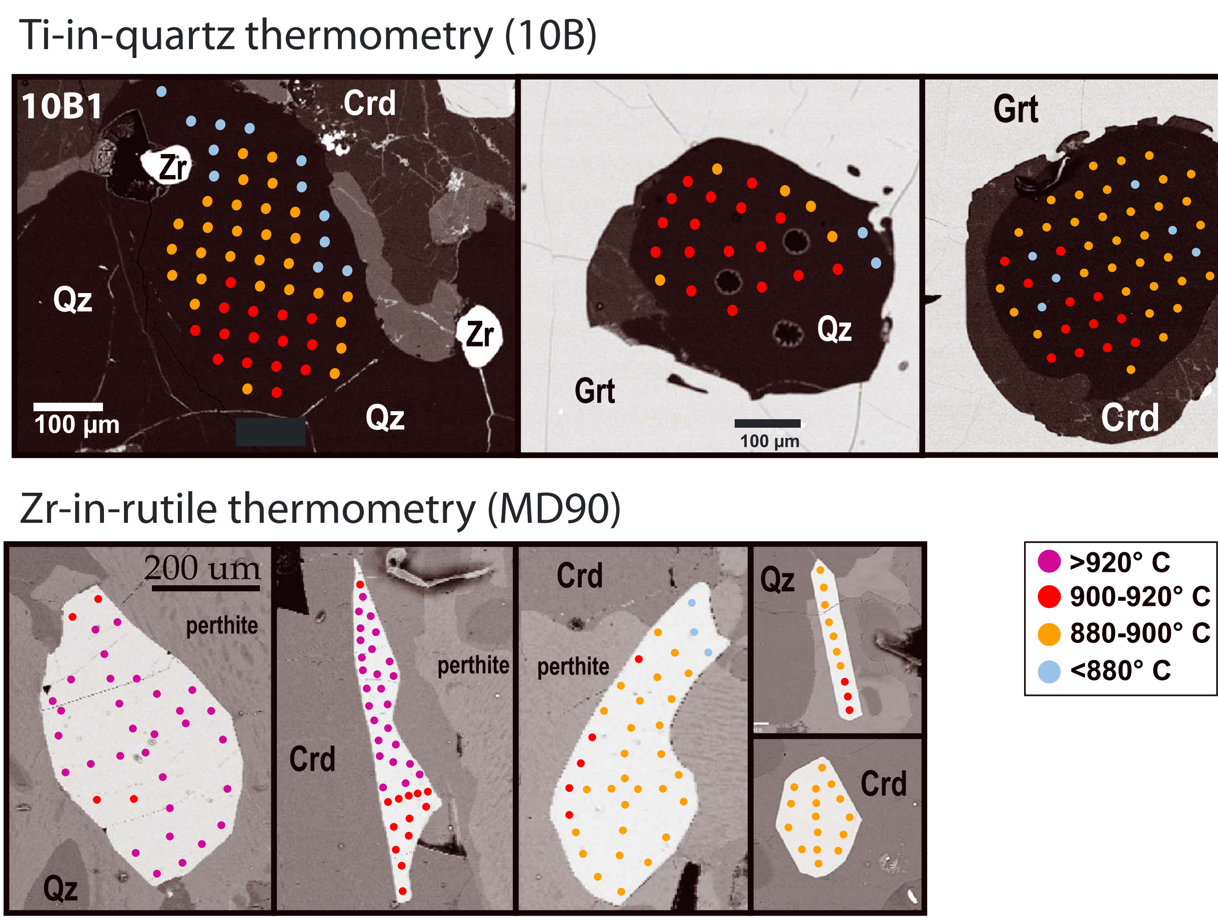

Figure 4. Representative electron backscatter grain maps showing 4+ cation thermometry results. Ti-in-quartz [after *Thomas et al.*, 2010] temperatures and Zr-in-rutile [after *Ferry and Watson*, 2007] temperatures were calculated assuming a pressure of 10 kbar.

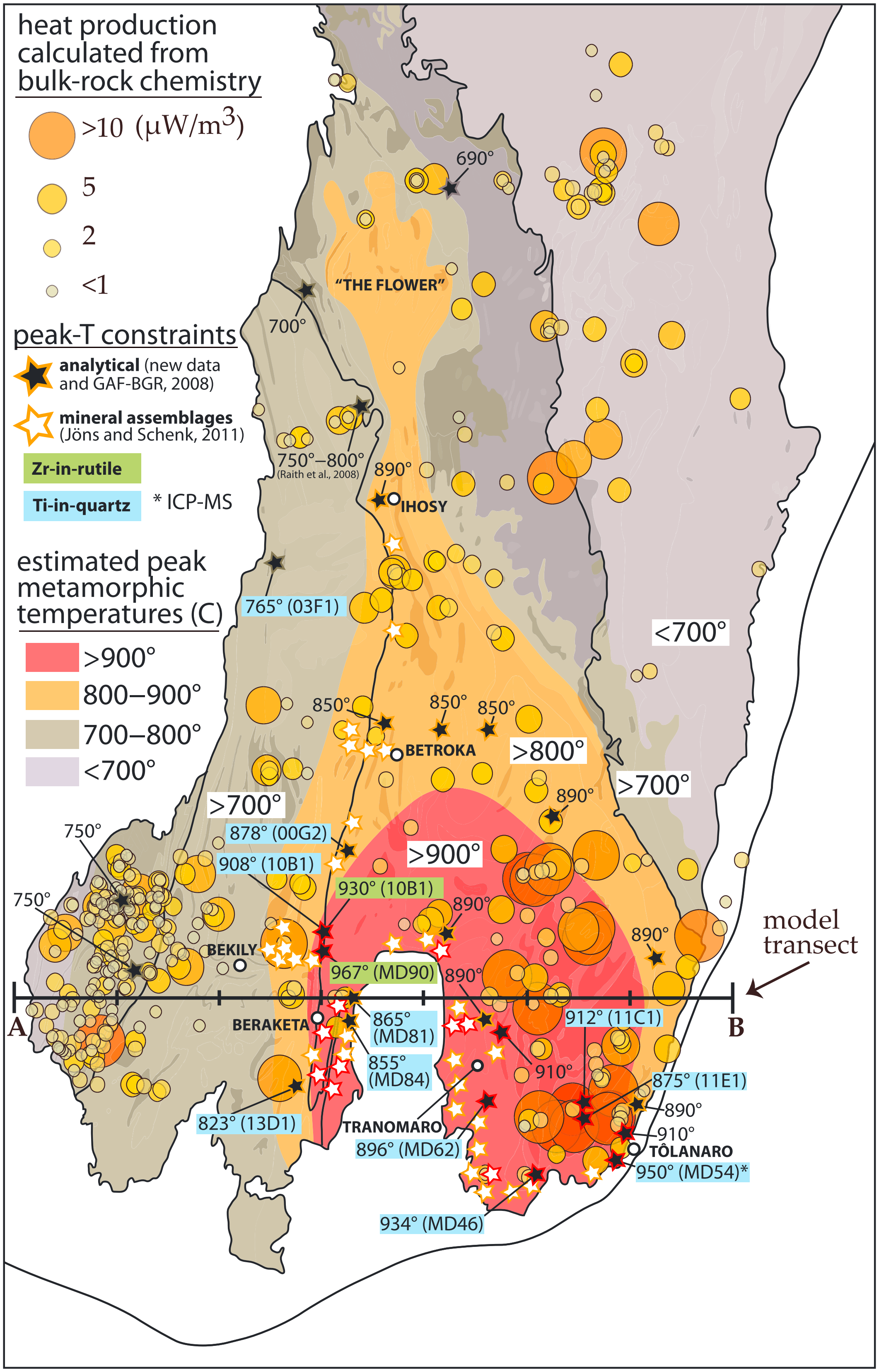

Figure 5. Map of southern Madagascar showing estimated peak isotherms based on mineral assemblages [*Jöns and Schenk*, 2008], pseudosections [*GAF-BGR*, 2008], and 4+ cation thermometry. Heat production rates (at 550 Ma) based on bulk rock chemistry [*GAF-BGR*, 2008] are plotted as shaded circles.

Table 2. Default Parameters for Thermal Modeling

Parameter	Value	Unit
Width	350	km
Height	150	km
Node spacing	2	km
Depth of crust	60	km
Lithosphere-asthenosphere boundary	150	km
Time step size	1	Myr
Duration of calculation	80	Myr
Thermal conductivity	3	W/m K
Basal heat flow	17	mW/m^2
Surface temperature	0	°C
Asthenosphere temperature	1350	°C
Erosion	0	km
Amount of thinning	0	km
RHP in uppermost crust	1.5	$\mu W/m^3$
Extrapolated depth of measured RHP	20 to 50	km
RHP in lowermost crust	0.7	$\mu W/m^3$
RHP in mantle	0.02	$\mu W/m^3$

assemblage of the Ampahiry formation (a similar bulk composition to the Bakika formation, but with a low ferric iron content) predicts maximum temperatures of 830°C. Because the Ampahiry formation is interlayered with the Bakika formation near Tôlanaro, both presumably experienced a similar PT history; *GAF-BGR* [2008] concluded that the Ampahiry rocks reached $>$830°C when biotite was absent, and that either (a) the biotite formed on the retrograde path or (b) the biotite solution model they used is inappropriate. Fortunately, the Ihosy formation exists throughout much of the Anosyen domain, providing thermal constraints across a large area (Figure 5).

4.2. The 4+ Cation Thermometry

We conducted Ti-in-quartz (using the calibration of *Thomas et al*. [2010]) and Zr-in-rutile [*Ferry and Watson*, 2007] thermometry for 13 samples (Tables 1 and S5 and Figures 4 and 5). Electron probe microanalysis (EPMA) and laser ablation ICP-MS were used to measure Ti and Zr in quartz and rutile, respectively, and calibrated using National Institute of Standards and Technology glass reference materials. EPMA 2σ uncertainty is $<$1% and ICP-MS 2σ uncertainty is ~5–8%. Each sample exhibits a wide range of intergrain and intragrain Ti and Zr concentrations (Figure 4). We are unable to say whether this resulted from (i) heterogeneity in Ti and Zr activity at the thin section scale, (ii) incomplete equilibration, (iii) diffusion during cooling, and/or (iv) grain growth during cooling. Calculated temperatures are minima because Si and Ti activities were assumed to be unity; this is a reasonable assumption for Si based on the presence of quartz in every sample, but Ti activity may have been significantly lower in samples without rutile (all except 10B1 and MD90). Because the Ti activity is unconstrained in most cases, we assume that the highest Ti concentration measured in each sample is representative of minimum peak conditions. We use a pressure of 10 kbar [*GAF-BGR*, 2008; *Jöns and Schenk*, 2011], realizing that the Ti-in-quartz temperatures are reduced by ~25°C per kbar and the Zr-in-rutile temperatures by $<$10°C per kbar.

Two rutile-bearing samples (10B1 and MD90) were collected from the southern Beraketa shear zone; both yield UHTM Zr-in-rutile temperatures (maxima of 930°C and 967°C, respectively). Grain 8 in 10B1 and grain 2 in MD90 have flat Zr concentration profiles (see Table S5) and yield the highest temperatures, suggesting that they are most representative of peak temperature [e.g., *Taylor-Jones and Powell*, 2015]. These two samples are considered the most robust evidence for UHTM in southern Madagascar because the rutile thermometer is less pressure dependent. Ti-in-quartz temperatures for 10B1 (EPMA) and MD90 (ICP-MS) are consistent with the Zr-in-rutile results, reaching 908°C (~925°C via ICP-MS) and 913°C, respectively; the discrepancy between maximum temperatures calculated for MD90 could be due to (a) differences in pressure or temperature of Ti and Zr entrapment, (b) diffusive loss of Ti from quartz (faster than Zr diffusion in rutile) [*Cherniak et al*., 2007], or (c) too few analyses. In general, however, the consistency among thermometers for these two samples seems to justify using 10 kbar for the Ti-in-quartz thermometer.

Ti-in-quartz temperatures calculated for other samples also indicate UHTM: MD54 collected near Tôlanaro gave ~950°C, MD46 to the west yielded 934°C, and 11C1 to the north gave 912°C. Samples 11E1 (875°C), MD62 (896°C), MD81 (865°C), and MD84 (855°C) yielded temperatures below 900°C; given their close proximity to higher-temperature rocks, however, these results may underestimate peak temperature. Two other samples along the Beraketa shear zone—00G2 (878°C) and 13D1 (823°C)—are from locations outside the zone of demonstrable UHTM. A sample from the northern Androyen domain (03 F1) has a lower maximum Ti-in-quartz temperature of 765°C, consistent with decreasing metamorphic grade to the north and west.

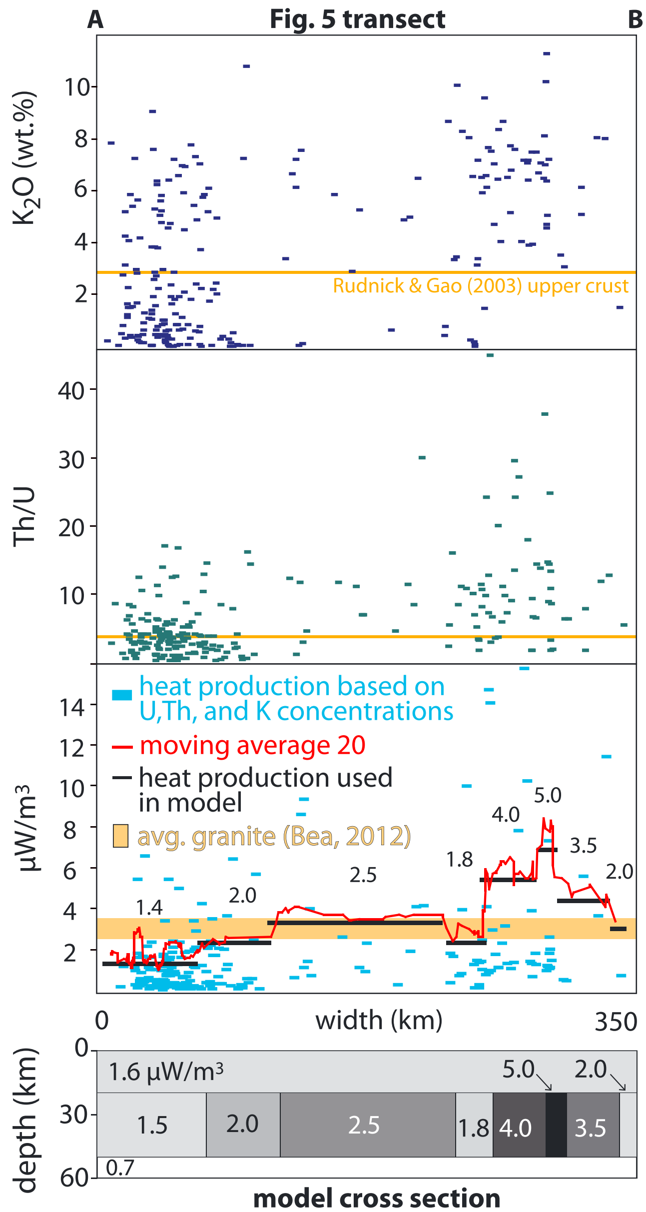

Figure 6. Heat-producing element distribution across southern Madagascar. Because lithologies are generally N-W trending, bulk rock samples south of 23°S were projected onto the A-B transect (see Figure 5). Segments of the transect were delineated using a 20-point central moving mean (red line) from A to B, and mean heat production for each segment was compiled and input into thermal models as a radiogenic layer in the middle crust.

5. Thermal Modeling

To evaluate the role of heat production in southern Madagascar, we use a 2-D transient heat flow model based on the alternating direction, implicit, finite-difference method described by *Hinojosa and Mickus* [2002]. The model is a 350×150 km rectangular grid with 2 km node spacing. The initial temperatures are steady state conditions for 40 km thick crust in which a 14 km thick upper crust has RHP of 1.6 μW/m^3 and the underlying 26 km has 0.7 μW/m^3; this is then instantaneously stretched vertically to 60 km to represent thickening. Thermal conductivity and crustal thickness (60 km) are constant in all model runs. Basal (mantle) heat flow is assumed to be constant and the surface temperature is held at 0°C. Time steps of 1 Myr are used; smaller steps yield nearly identical results. There is no material flow, except for simulations in which the node temperatures and RHP values are shifted upward to simulate erosion. Default parameters are listed in Table 2.

5.1. Heat Production

To simulate burial of radiogenic crust during continental collision, a high-RHP layer is inserted into the middle to lower crust. Thermobarometric constraints for the Anosyen domain suggest that the high-RHP layer exposed now came from depths of 18 to 30 km (pressures of 6–6.5 kbar or 9–10 kbar) [*Boger et al.*, 2012; *GAF-BGR*, 2008; *Jöns and Schenk*, 2011], so the high-RHP layer is inserted at 20 km depth. RHP above that is assumed to be 1.6 μW/m^3. Below the high-RHP layer, the RHP of the lower crust (to 60 km depth) and mantle (to 150 km depth) are 0.7 μW/m^3 and 0.02 μW/m^3, respectively. The composition of the RHP layer is approximated based on *GAF-BGR* [2008] bulk-rock analyses (Table S6). A heat production rate is calculated for each sample based on elemental abundances (corrected for 550 Myr of decay) and heat production rates of U (97.1 μW/kg), Th (26.9 μW/kg), and K (3.58 nW/kg). The individual heat production values south of 23°S longitude are then projected onto an E-W transect (Figure 6) orthogonal to the dominant N-S structural trend. This transection is divided into eight segments with different average RHP rates. The RHP values remain constant throughout the simulations (i.e., HPEs are not moved from node to node due to melting or fluid migration), except when erosion removes the uppermost crust and the RHP values are shifted upward.

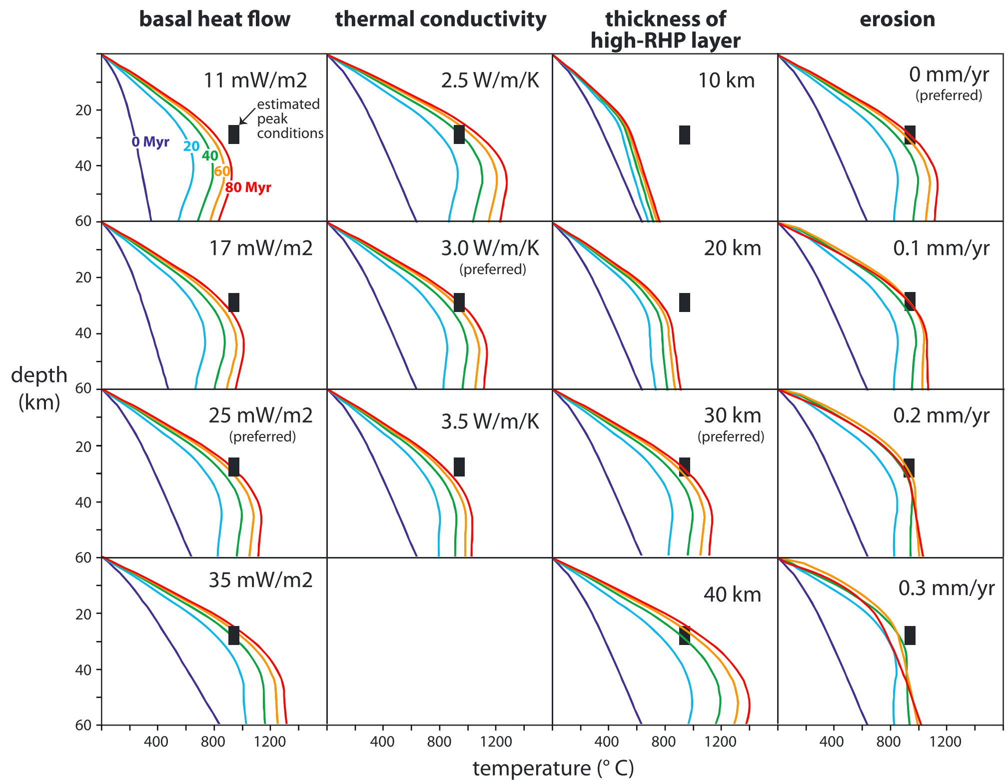

Figure 7. Sensitivity tests for various thermal model parameters. The geotherm plotted is 275 km east of A on the model transect (Figures 5 and 6), and the black rectangle represents estimated peak conditions for the UHTM zone in southern Madagascar. Note that heating is asymmetric and that the geotherm plotted represents the hottest segment of the thermal model. See text for details.

5.2. Thickness of the Heat-Producing Layer

Because sample-based RHP values are higher than those in the upper and lower crust—by as much as a factor of 5—the thickness of the high-RHP layer strongly affects the model. The thickness of the layer was varied from 10 to 40 km in different simulations. Highly radiogenic crustal layers thicker than ~25 km produce UHT at 30 km depth in <60 Myr (Figure 7).

5.3. Mantle Heat Flux

The model is sensitive to mantle heat flux. Continental mantle heat flux is typically estimated by subtracting presumed heat production within the crust from the surface heat flow. Estimates vary greatly from 7 to 25 mW/m^2 for various continental regions; most are 12–18 mW/m^2 [*Mareschal and Jaupart*, 2013, and references therein]. We explore the influence of mantle heat flow by varying it from 11 to 23 mW/m^2. In the model, higher mantle heat flow raises the initial geotherm, producing higher temperatures sooner (Figure 7). A moderate heat flow of 17 mW/m^2 is used as the preferred value.

5.4. Thermal Conductivity

The rate of heating is also sensitive to thermal conductivity, which depends on mineralogy [e.g., *McLaren et al.*, 1999; *Hofmeister et al.*, 2006] and temperature [e.g., *Whittington et al.*, 2009]. The bulk thermal conductivity measured for felsic, intermediate, and mafic granulites across southern India ranges from 2.4 to 3.5 W/m/K [*Ray et al.*, 2015]; rocks in southern Madagascar are likely similar. The conductivity of rocks in the now-eroded upper crust is unknown; we test constant conductivities of 2.5, 3.0, or 3.5 W/m/K. Lowering conductivity accelerates heating by insulating the heat-producing layer (Figure 7); we consider a conservative conductivity of 3.0 W/m/K to be typical but acknowledge that the middle and lower crust must have had lower conductivities after heating above ~600°C, especially if partial melt persisted for extended periods [e.g., *Whittington et al.*, 2009].

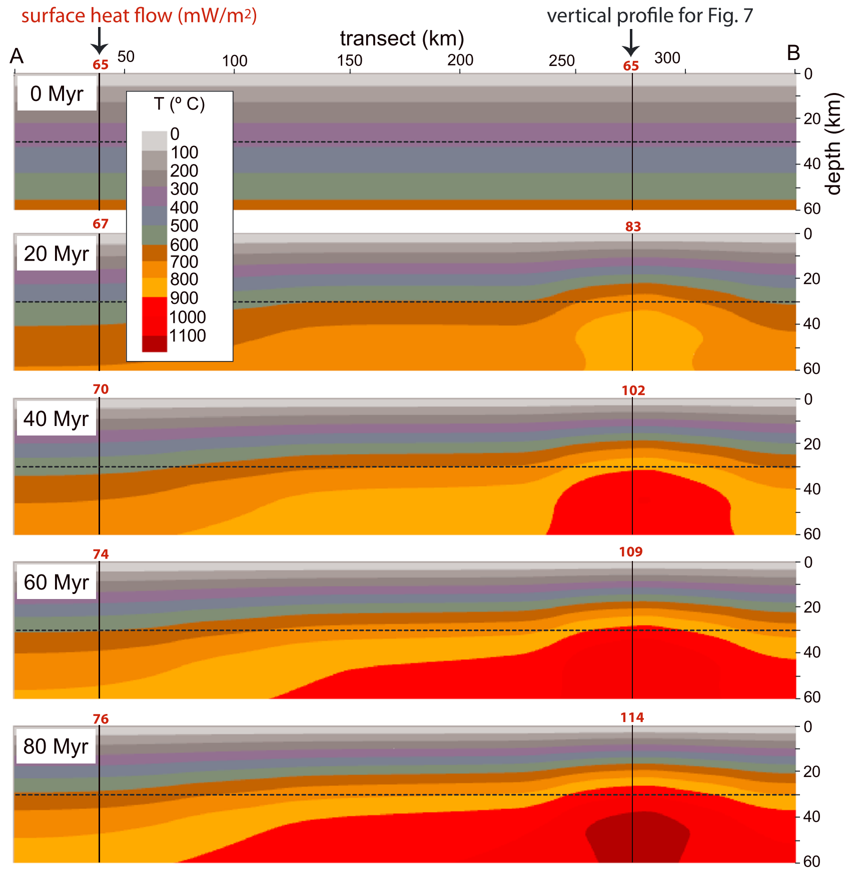

Figure 8. Time slices for the preferred parameterization of the model (see text for justification). Approximately 60 Myr is necessary to reproduce temperatures at 30 km depth that are representative of peak conditions across southern Madagascar.

5.5. Erosion

Erosion influences heating by changing the distribution of HPEs and advecting heat upward. Denudation rates <0.1 mm/yr do not significantly affect the thermal evolution of the middle crust (Figure 7). In contrast, erosion rates of 0.2 mm/yr accelerate heating >2°C/Myr for the first 20 Myr. An even faster erosion rate of 0.3 mm/yr (18 km in 60 Myr) transfers the high-HPE layer into the less insulated upper crust, resulting in peak temperatures colder than observed. The Tibetan plateau—the best modern analogue for the Pan-African collision zone—has experienced slow regional denudation rates of ~0.01–0.03 mm/yr [*Lal et al.*, 2004; *Hetzel et al.*, 2011]. If denudation of the Pan-African orogen was analogous to Tibet, erosion probably had a negligible effect on the overall thermal evolution of the central part of the orogen. We use an erosion rate of zero to approximate slow denudation of the orogenic plateau.

5.6. Crustal Thinning

Crustal thinning that outpaces conduction compresses the geotherm. For example, exhumation of lower crustal rocks at >900°C to midcrustal depths could explain the type of UHTM seen in southern Madagascar. Although most of the Tibetan plateau is thickening [*Liang et al.*, 2013], some portions, such as the southeastern portion between the eastern syntaxis and the Sichuan basin [*Enkelmann et al.*, 2006] may by thinning in response to outward directed flow [e.g., *Clark and Royden*, 2000].

5.7. Timescale of Heating

Burial of radiogenic rocks to depths of 30 km presumably occurred due to tectonic thickening of the crust. It remains unclear whether and to what extent the accretion of the Vohibory Arc caused thickening of the crust prior to 600 Ma. Magmatism and metamorphism occurred across hundreds of kilometers from ~580 to 515 Ma, which is consistent with the existence of a thickened orogenic plateau for ~65 Myr. Without conclusive evidence of prior tectonic burial of the UHTM terrane, we assume that heating occurred for approximately 60 Myr.

5.8. Successful Models

A successful model must replicate the UHT conditions across a 150 km wide zone in the middle crust within ~65 Myr. We evaluated the model at 30 km depth but acknowledge that the exposed UHT rocks in Madagascar may have resided at shallower depths. By extending the thickness of the heat-producing layer from 20 km to 50 km depth and assuming reasonable mantle heat flow and thermal conductivity values of 25 mW/m^2 and 3.0 W/m/K, respectively, the highest heat-producing segments of the model (southern Anosyen domain) reach 900°C at a depth of 30 km in <60 Myr and the geotherm becomes inverted in the lowermost crust. Heating across the model transect is strongly asymmetric (Figure 8): in the west (Vohibory domain), temperatures remain below 700°C in the middle crust, even after 60 Myr. Surface heat flow in this scenario increases from 65 to 76 mW/m^2 in the west and from 65 to 114 mW/m^2 in the east; these values are within the range observed across the Tibetan plateau (30–140 mW/m^2) [*Hu et al.*, 2000]. A lower thermal conductivity (~2.5 W/m/K) or a thicker highly radiogenic layer (~40 km thick) cause UHTM in the east in <40 Myr. Conversely, if the highly radiogenic layer is <25 km thick or if it resided in the upper 30 km of the crust, UHTM is not reached in <80 Myr. Lower mantle heat flow and/or rapid erosion would have also moderated heating.

6. Discussion

6.1. Tectonometamorphic Evolution of Southern Madagascar

The lack of consensus about the timing of orogenesis in southern Madagascar has been due in part to analytical techniques that dated only single metamorphic grains or bulk separates, and in part to the long, complex orogenic cycle. Our data shed new light on several critical aspects of the continental collision.

The presence of inherited Paleoproterozoic monazite and zircon that are not detrital indicates that much, perhaps all, of the Anosyen domain metasedimentary rock was deposited prior to ~2 Ga [e.g., *Tucker et al.*, 2014] rather than during the Neoproterozoic [e.g., *GAF-BGR*, 2008]. However, volcanogenic beds derived from Neoproterozoic arc magmatism may have been deposited on those Paleoproterozoic metasedimentary rocks and then been structurally interleaved during collision.

A pre-600 Ma metamorphic event affected both the Androyen domain and western Anosyen domain. Monazite that grew during this older event ranges from 622 ± 13 Ma (13D1) to 593 ± 13 Ma (00G2) and exhibits textures and trace element signatures indicative of garnet-absent growth (high Lu/Dy and Y) in the presence of melt (oscillatory zoning) (Figure 2); the distinctive monazite trace element signature and limited spatial extent of an early ~600 Ma event are compatible with an accretion of the Vohibory arc to the Androyen and Anosyen domains prior to 620 Ma [e.g., *de Wit et al.*, 2001] and well before the onset of the East-West Gondwana collision. We cannot rule out, however, that the Vohibory and Androyen/Anosyen domains were already attached to their respective East and West Gondwana margins prior to this event. Whether the Androyen and Anosyen domains were thickened—and remained so—by this event is difficult to quantify due to subsequent reworking. We speculate that the juxtaposition of hot arc rocks next to the Androyen domain heated the continental margin to the solidus along a counterclockwise pressure-temperature path before crust became especially thick. This is compatible with immature-arc magmatism in the Vohibory domain until ~630 Ma [*GAF-BGR*, 2008] and monazite growth in the presence of melt less than 10 Myr later within the Androyen and Anosyen domains.

The existence of pre-600 Ma metamorphic dates in the Anosyen domain contradicts the tectonic model proposed by *GAF-BGR* [2008] in which the final suturing of East and West Gondwana occurred along the contact between the Androyen and Anosyen domains after 600 Ma. Furthermore, it is difficult to reconcile the existence of a west facing ~850–700 Ma continental arc that produced the Imorona-Itsindro suite [*Müller*, 2000; *GAF-BGR*, 2008; *Moine et al.*, 2014; *Ichiki et al.*, 2015] with a model in which outboard terranes (i.e., Androyen and Anosyen domains) were contiguous with older cratonic portions of East Gondwana since the Paleoproterozoic [e.g., *Tucker et al.*, 2014]. Rather, the inferences that the Vohibory arc was oceanic until ~630 Ma and that the Imorona-Itsindro magmatism (until ~700 Ma) represents an east directed subduction of oceanic crust necessitate that there were oceans on both sides of an Androyen-Anosyen microcontinent prior to final Gondwana assembly. Regardless of whether the Antananarivo domain was part of the hypothesized Azania microcontinent [*Collins and Pisarevsky*, 2005; *Collins*, 2006] or East Gondwana [*Tucker et al*., 2014], a separate Androyen-Anosyen microcontinent must have existed to the west.

The timing of final suturing of the Androyen-Anosyen domains to East and West Gondwana remains uncertain. On the western edge of the Androyen domain, garnet-present monazite growth may have started as early as ~590 Ma (14G1), but most analyses with low heavy rare earth element abundances (compatible with garnet in the rock) occur after 570 Ma (Figure 2). Whether there was a 10–20 Myr tectonic/metamorphic hiatus after arc accretion cannot be resolved with the chronologic precision achieved in this study. However, the ubiquitous metamorphic dates and Ambalavao granite intrusions across southern Madagascar beginning at 580–570 Ma [e.g., *Tucker et al*., 2014] suggest that the main stage of continental collision began prior to this time. The central and northern parts of the Antananarivo domain did not experience metamorphism and magmatism until ~560 Ma, compatible with ~100–200 km northeastward propagation of the orogen during a span of 10–20 Myr. We envisage that continent-continent collision metamorphism occurred first within a moderately prethickened and recently active western margin of an Androyen-Anosyen microcontinent, after which regional metamorphism extended eastward at a rate commensurate with eastward crustal thickening.

Previously published petrology and our new 4+ thermometry allow us to map peak isotherms in detail (Figure 5); by assuming that mineral assemblage constraints and quantitative thermometry are lower bounds for peak metamorphic temperatures, spatially coherent thermal zones emerge from the data. UHTM affected a 150 km wide zone in the southern Anosyen domain (and probably the southeasternmost Androyen domain) between Beraketa and Tôlanaro; the north-south extent of UHTM may have been $>$150 km as well and probably extends into southern India, Sri Lanka, and Antarctica. In Madagascar alone, UHTM influenced $>$20,000 km^2. Nearly all of the Anosyen domain and the eastern Androyen domain experienced temperatures in excess of 800°C. The decreasing thermal field gradient to the north ($<$1°C/km) in the northern Anosyen domain was probably accompanied by a slight decrease in peak pressures [*GAF-BGR*, 2008; *Jöns and Schenk*, 2011]. The peak metamorphic gradients are steeper ($>$2°C/km) to the east and west, but it is unclear to what extent these have contracted during shearing along the Ranotsara and Beraketa shear zones. Nevertheless, the Anosyen domain reached peak temperatures that were considerably hotter at comparable depths than in the adjacent domains to the east and west. This phenomenon cannot be explained entirely by postpeak-metamorphic rejuxtaposition, because there is no evidence of large vertical displacements in southern Madagascar. Notably, peak temperatures do not correlate spatially with the Vohibory arc and occurred $>$50 Myr after arc accretion, which suggests that the arc was not the principal heat source.

Across southern Madagascar, metamorphic growth of monazite and zircon ended between 525 Ma and 515 Ma during postdeformation Ambalavao granite emplacement. Regional decompression [e.g., *Jöns and Schenk*, 2011], as well as the coeval cessation of metamorphism, magmatism, and deformation, is consistent with N-S extensional collapse of the orogen [e.g., *Dewey*, 1988] perpendicular to the E-W Gondwanan convergence. The southern Anosyen domain was extruded southward as a somewhat-cohesive crustal wedge [e.g., *Martelat et al*., 2000; *Schreurs et al*., 2010], whereas the northern Anosyen domain was extruded northward, flowing into a “flower” shape [e.g., *Tucker et al*., 2014]. Cooling of the UHTM domain was probably accommodated by exhumation to shallower crustal depths and the extraction of granite melts.

6.2. The Role of Radiogenic Heat Production

Bulk-rock HPE concentrations indicate that the Anosyen domain has RHP rates much higher than average Proterozoic crust (0.73–0.90 μW/m^3) [*Jaupart and Mareschal*, 2003]. Moreover, some metasedimentary rocks in southern Madagascar are more radiogenic than HPE-rich granites, the conventional culprit for heterogeneous heat production [e.g., *McLaren et al*., 1999; *Bea*, 2012; *McLaren and Powell*, 2014]. Assuming that bulk-rock-based rates represent heat production in the middle crust during orogenesis, static models produce ultrahigh temperatures at 30 km depth and at length scales and over timescales similar to that of the UHTM zone in southern Madagascar (Figures 5, 7, and 8). Considering that the models reproduce an E-W geothermal gradient comparable to that observed in Madagascar in a time frame compatible with geochronologic constraints, radioactive decay was probably the primary control on the thermal evolution of the middle crust. For this to be the case, however, several conditions must have been met. First, the highly radiogenic layer must have been at least ~25 km thick and resided at $>$20 km depth for the duration of heating. If U were removed from this layer during melting and granite magmatism, however, the RHP could have been even higher and a thinner radiogenic layer would have provided sufficient heat. Either way, heat production would have been severely limited if denudation removed >20 km of the upper crust. Second, the upper crust above the highly radiogenic layer must have provided sufficient insulation, probably requiring an average thermal conductivity of 3.0 W/m/K or less. Third, heat flow from the mantle as low as 11 mW/m^2 may have been sufficient for UHTM to occur within 65 Myr. Lastly, surface heat flow during UHTM in the middle crust must have been very high, probably exceeding 100 mW/m^2.

Although focused RHP appears to have been the primary driver of UHTM in southern Madagascar, other heat sources may have contributed. For example, the accretion of the Vohibory arc to the Androyen domain likely caused regional heating, and the geothermal gradient may not have relaxed entirely prior to the main stage of orogenesis. However, the peak UHT temperatures were not reached adjacent to the Vohibory domain, indicating that heat from the arc was not the primary cause for UHTM. At temperatures less than 600°C, mechanical heat production could have been significant: doubling the thickness of crust with a density of 2700 kg/m^3 and specific heat of 1000 J/kg/K theoretically increases temperature by 37°C [*Stüwe*, 2007]. In most modeled scenarios, however, temperatures in the Anosyen domain reach 600°C in <20 Myr, after which mechanical heating would have become inconsequential due to thermal weakening. Changes in the mantle heat flux are also potentially important; as noted by *Bea* [2012], a modest increase in heat flux from the mantle due to lithospheric delamination, mantle wedge convection, or ponding of deep magma would have exaggerated heating of crust with elevated heat production. Seismic data from the Tibetan Plateau suggest that asthenosphere is upwelling in response to the delamination of mantle lithosphere beneath Tibet and the rollback of the subducting Indian slab [*Shi et al*., 2015]. There is no evidence in southern Madagascar that the UHTM was caused by heat advection by mantle magmas. Charnockites in the Anosyen domain [e.g., *Jöns and Schenk*, 2011] are generally felsic [*GAF-BGR*, 2008], so even if they are igneous, their low heat capacities would have limited the extent to which they could transfer heat from the mantle.

Concentrated RHP in southern Madagascar caused an extreme thermal anomaly in the middle crust: Our results demonstrate that the heterogeneous distribution of HPEs in southern Madagascar led to asymmetric heating, with a difference between the cool and hot segments of the model of up to 300°C at 30 km depth. Because rock strength is temperature dependent, focused RHP would have caused focused weakening of the crust. Without taking into account melt weakening, an increase in temperature at the base of a crustal column by 100°C can lead to a reduction in bulk strength by a factor of 2–3 [*Sandiford and McLaren*, 2002]. The southern Anosyen domain undoubtedly underwent even greater thermal weakening, but precise estimates of strength are difficult due to the complex lithologic heterogeneity of the region and the potential role of melt weakening. It is possible that the thermal weakening exceeded the threshold of gravitational stability of the thickened crust [e.g., *Lexa et al*., 2011], causing extensional collapse of the orogen [e.g., *Dewey*, 1988] that was accommodated by the N-S extrusion of the Anosyen domain from 525 to 515 Ma.

6.3. (Re)Distribution of Heat-Producing Elements

Compared to the model upper continental crust of *Rudnick and Gao* [2003, 2014], the southern Anosyen samples have, on average, roughly the same amount of U (2.7 ppm), one and a half times as much K (4.2 wt %), and 4–5 times as much Th (51 ppm). For typical crustal Th/U ratios of 4 to 1, Th and U produce similar amounts of heat: At 550 Ma, the *Rudnick and Gao* [2003] upper crustal abundances of U, Th, and K would have produced roughly 41%, 39%, and 19% of the total heat production, respectively. Samples from southern Madagascar have much higher average Th abundances, such that Th produced nearly 75% of the heat, with U and K producing 15% and 10%, respectively.

The mobility of U and Th during metamorphism is largely controlled by the stability of accessory phases [*Rudnick and Presper*, 1990]. Of the Th- and U-bearing phases in high-grade metamorphic rocks, monazite is especially important because apatite is more soluble in felsic melts [*Wolf and London*, 1995] and xenotime is consumed during prograde garnet growth [*Bea and Montero*, 1999]. Zircon can be stable under granulite-facies conditions, but typically has much lower U and Th concentrations than monazite (most zircon has >2 orders of magnitude less Th). During partial melting, monazite solubility in peraluminous granitic melt depends on the light rare earth element (LREE) concentration of the source [*Rapp and Watson*, 1986], but in most cases LREE saturation probably prevents the complete dissolution of monazite at temperatures below ~800°C [*Rapp et al*., 1987] and favors monazite retention in the residue. Anhydrous melting [*Watt* *and Harley*, 1993] or metamorphism [*Bingen and van Breemen*, 1998] of metapelite at higher temperatures can also result in residual monazite. Thus, monazite tends to be retained in the residue when (i) the source contains high initial concentrations of LREEs or P that can saturate the melt; (ii) monazite growth precedes partial melting; (iii) hydrous melting occurs at less than ~800°C; and/or (iv) melts and fluids that react with the rock above ~800°C are anhydrous.

U is generally more mobile than Th during metamorphism and melting because lattice-bound U^{4+} can be oxidizing into soluble U^{6+} and mobilized by fluids and melts. Granulite terranes typically are depleted in U [*Reid et al*., 1989; *Rudnick and Presper*, 1990], especially when monazite is present [*Bea and Montero*, 1999]. Monazite grown during high-temperature metamorphism tends to have high Th/U [e.g., *Bingen and van Breemen*, 1998] because U is preferentially retained in melt or metamorphic fluid, whereas Th is incorporated into monazite. In Madagascar, Paleoproterozoic metamorphism led to monazite growth in the Androyen and Anosyen domains (e.g., sample 06C1), effectively preconditioning the crust by armoring the Th in relatively large grains. During Gondwana amalgamation, partial melting probably occurred at $<$800°C or under anhydrous conditions that were unfavorable for monazite dissolution. High-temperature metamorphism dissolved some preexisting monazite, but the prevalence of metamorphic monazite rims suggests that a significant fraction of dissolved monazite was reprecipitated on older grains rather than being extracted from the middle crust. If U was extracted during melting and metamorphism, the bulk rock analyses used to calculate the RHP may be underestimates for the early stages of orogenesis. Conversely, if Th became concentrated the melt residue, focused RHP may have been delayed until after melt extraction. Depending on initial abundances, complementary depletion of U and enrichment of Th may have left the total heat production relatively unchanged [e.g., *Bea and Montero*, 1999].

Melt extraction tends to lower the U concentration of the melt residue, yet southern Anosyen migmatitic residues contain U concentrations comparable to average crust. It seems probable, therefore, that metasedimentary protoliths were U- and Th-rich prior to orogenesis. Globally, sedimentary rocks increase in bulk U by a factor of $>$2 and increase in Th by a factor of $>$3 at the Archean-Proterozoic transition [*McLennan et al*., 1980], just prior to the deposition of the Anosyen domain. This sedimentary enrichment may have been caused by unprecedented late Archean intracrustal melting and potassic granitic magmatism that transported large volumes of U and Th to the upper crust [*McLennan et al*., 1980]. Additionally, Paleoproterozoic subaerial exposure and oxidative weathering of Anosyen protoliths could have caused premetamorphic fractionation of Th and U; high U concentrations in shales indicate that from 2.4 Ga to 2.0 Ga, oxidative weathering on the continents preferentially transported U to the oceans [*Partin et al*., 2013].

7. Conclusions

Our geochronologic results elucidate the protracted tectonic history of the UHTM domain exposed in southern Madagascar: rocks that were metamorphosed in the Paleoproterozoic collided with the Vohibory arc at ~630 Ma, after which the collision between East and West Gondwana thrust them into thickened crust by ~580 Ma. New quantitative thermometry helps delineate a broad zone of UHTM, almost entirely in the southern Anosyen domain. RHP rates calculated from bulk rock compositions suggest that heat production was sufficiently high to explain UHTM within 65 Myr if the radiogenic layer was at least 25 km thick, leading us to surmise that RHP was the principal source of heat responsible for the UHTM. Moreover, focused heating caused by very high Th concentrations can explain why peak temperatures were much higher in the east. We conclude that the initial enrichment in HPEs, prior metamorphism, and the resiliency of monazite during orogenesis allowed enough Th to be retained to eventually cause UHTM.

Although neglected in most numerical models, accessory phase stability and heterogeneous HPE distributions in the crust may exert major influence on the thermomechanical evolution of orogens. Over long timescales, thickened crust can only be maintained if average crustal heat production is low and if HPEs are concentrated in the uppermost crust [e.g., *Sandiford and McLaren*, 2002; *Mareschal and Jaupart*, 2013]; in lieu of magmatic/metasomatic redistribution of HPEs or rapid surface denudation, long-term stability of the crustal column may be attained if HPE-rich domains are transferred structurally to shallower depths. Extreme temperatures, thermal weakening and gravitational collapse—such as the exhumation of the Anosyen domain—may be the inevitable result of HPEs trapped in the lower portions of tectonically thickened crust. Until we better understand why and how HPEs are mobilized during high-temperature processes, the extent to which RHP governs orogenic dynamics will remain uncertain. Microanalysis of metamorphic monazite—a major host of Th as well as a datable accessory mineral—shows promise as a way of tracking HPEs. Monazite stability under various high-temperature conditions deserves renewed attention, both experimentally and in regional metamorphic studies.

Acknowledgments
This research was funded by NSF EAR-1348003 and a NSF Graduate Research Fellowship awarded to F. Horton. Volker Schenk generously provided samples. We thank Professor Michel Rakotondrazafy and his graduate students Jeremia Ramarijaona and Laurent Rakotondramanana for their exemplary help in the field. We also thank Simon Harley for his thoughtful review of this manuscript. All data are available upon request from the corresponding author.

References

Annen, C., J. D. Blundy, and R. S. J. Sparks (2006), The genesis of intermediate and silicic magmas in deep crustal hot zones, *J. Petrol.*, *47*(3), 505–539.

Bea, F. (2012), The sources of energy for crustal melting and the geochemistry of heat-producing elements, *Lithos*, *153*, 278–291.

Bea, F., and P. Montero (1999), Behavior of accessory phases and redistribution of Zr, REE, Y, Th, and U during metamorphism and partial melting of metapelites in the lower crust: An example from the Kinzigite formation of Ivrea-Verbano, NW Italy, *Geochim. Cosmochim. Acta*, *63*(7), 1133–1153.

Beaumont, C., R. A. Jamieson, M. H. Nguyen, and S. Medvedev (2004), Crustal channel flows: Numerical models with applications to the tectonics of the Himalayan-Tibetan orogen, *J. Geophys. Res.*, *109*, B0406, doi:10.1029/2003JB002809.

Beaumont, C., R. Jamieson, and M. Nguyen (2010), Models of large, hot orogens containing a collage of reworked and accreted terranes, *Can. J. Earth Sci.*, *47*(4), 485–515.

Behn, M. D., P. B. Kelemen, G. Hirth, B. R. Hacker, and H.-J. Massonne (2011), Diapirs as the source of the sediment signature in arc lavas, *Nat. Geosci.*, *4*, 641–646.

Berger, A., E. Gnos, G. Schreurs, A. Fernandez, and M. Rakotondrazafy (2006), Late Neoproterozoic, Ordovician and Carboniferous events recorded in monazites from southern-central Madagascar, *Precambrian Res.*, *144*(3), 278–296.

Bingen, B., and O. van Breemen (1998), U-Pb monazite ages in amphibolite-to granulite-facies orthogneiss reflect hydrous mineral breakdown reactions: Sveconorwegian Province of SW Norway, *Contrib. Mineral. Petrol.*, *132*(4), 336–353.

Boger, S. D., R. W. White, and B. Schulte (2012), The importance of iron speciation (Fe^{2+}/Fe^{3+}) in determining mineral assemblages: An example from high-grade aluminous metapelites of southern Madagscar, *J. Metamorph. Geol.*, *30*, 997–1018.

Boger, S. D., W. Hirdes, C. A. M. Ferreira, B. Schulte, T. Jenett, and C. M. Fanning (2014), From passive margin to volcano-sedimentary forearc: The Tonian to Cryogenian evolution of the Anosyen domain of southeastern Madagascar, *Precambrian Res.*, *247*, 159–186.

Brown, M. (2008), Characteristic thermal regimes of plate tectonics and their metamorphic imprint throughout Earth history: When did Earth first adopt a plate tectonics mode of behavior, *Geol. Soc. Am. Spec. Pap.*, *440*, 97–128.

Burg, J.-P., and T. V. Gerya (2005), The role of viscous heating in Barrovian metamorphism of collisional orogens: Thermomechanical models and application to the Lepontine Dome in the Central Alps, *J. Metamorph. Geol.*, *23*(2), 75–95.

Cherniak, D. J., E. B. Watson, and D. A. Wark (2007), Ti diffusion in quartz, *Chem. Geol.*, *236*(1), 65–74.

Clark, C., I. C. W. Fitzsimons, D. Healy, and S. L. Harley (2011), How does the continental crust get really Hot?, *Elements*, *7*(4), 235.

Clark, C., D. Healy, T. Johnson, A. S. Collins, R. J. Taylor, M. Santosh, and N. E. Timms (2014), Hot orogens and supercontinent amalgamation: A Gondwanan example from southern India, *Gondwana Res.*, *28*, 1310–1328, doi:10.1016/j.gr.2014.11.005.

Clark, M. K., and L. H. Royden (2000), Topographic ooze: Building the eastern margin of Tibet by lower crustal flow, *Geology*, *28*(8), 703–706.

Collins, A. S. (2006), Madagascar and the amalgamation of Central Gondwana, *Gondwana Res.*, *9*(1), 3–16.

Collins, A. S., and S. A. Pisarevsky (2005), Amalgamating eastern Gondwana: The evolution of the Circum-Indian Orogens, *Earth Sci. Rev.*, *71*(3–4), 229–270.

Collins, A. S., and B. F. Windley (2002), The tectonic evolution of central and northern Madagascar and its place in the final assembly of Gondwana, *J. Geol.*, *110*(3), 325–339.

Collins, A. S., P. D. Kinny, and T. Razakamanana (2012), Depositional age, provenance and metamorphic age of metasedimentary rocks from southern Madagascar, *Gondwana Res.*, *21*(2), 353–361.

Collins, A. S., C. Clark, and D. Plavsa (2014), Peninsular India in Gondwana: The tectonothermal evolution of the Southern Granulite terrain and its Gondwanan counterparts, *Gondwana Res.*, *25*(1), 190–203.

Currie, C. A., and R. D. Hyndman (2006), The thermal structure of subduction zone back arcs, *J. Geophys. Res.*, *111*, B08404, doi:10.1029/2005JB004024.

de Wit, M. J. (2003), Madagascar: Heads it's a continent, tails it's an island, *Annu. Rev. Earth Planet. Sci.*, *31*(1), 213–248.

de Wit, M. J., S. A. Bowring, L. D. Ashwal, L. G. Randrianasolo, V. P. Morel, and R. A. Rambeloson (2001), Age and tectonic evolution of Neoproterozoic ductile shear zones in southwestern Madagascar, with implications for Gondwana studies, *Tectonics*, *20*(1), 1–45, doi:10.1029/2000TC900026.

Dewey, J. F. (1988), Extensional collapse of orogens, *Tectonics*, *7*(6), 1123–1139, doi:10.1029/TC007i006p01123.

Dewey, J. F., L. Robb, and L. Van Schalkwyk (2006), Did Bushmanland extensionally unroof Namaqualand?, *Precambrian Res.*, *150*(3), 173–182.

Dufek, J., and G. W. Bergantz (2005), Lower crustal magma genesis and preservation: A stochastic framework for the evaluation of basalt–crust interaction, *J. Petrol.*, *46*(11), 2167–2195.

Emmel, B., N. Jöns, A. Kröner, J. Jacobs, J.-A. Wartho, V. Schenk, T. Razakamanana, and A. Austegard (2008), From closure of the Mozambique ocean to Gondwana breakup: New evidence from geochronological data of the Vohibory terrane, Southwest Madagascar, *J. Geol.*, *116*(1), 21–38.

England, P. C., and A. B. Thompson (1984), Pressure-temperature-time paths of regional metamorphism I. Heat transfer during the evolution of regions of thickened continental crust, *J. Petrol.*, *25*(4), 894–928.

Enkelmann, E., L. Ratschbacher, R. Jonckheere, R. Nestler, M. Fleischer, R. Gloaguen, B. R. Hacker, Y. Q. Zhang, and Y.-S. Ma (2006), Cenozoic exhumation and deformation of northeastern Tibet and the Qinling: Is Tibetan lower crustal flow diverging around the Sichuan Basin?, *Geol. Soc. Am. Bull.*, *118*(5–6), 651–671.

Ferry, J. M., and E. B. Watson (2007), New thermodynamic models and revised calibrations for the Ti-in-zircon and Zr-in-rutile thermometers, *Contrib. Mineral. Petrol.*, *154*(4), 429–437.

Foster, G., P. Kinny, D. Vance, C. Prince, and N. Harris (2000), The significance of monazite U–Th–Pb age data in metamorphic assemblages; A combined study of monazite and garnet chronometry, *Earth Planet. Sci. Lett.*, *181*, 327–340.

Foster, G., H. D. Gibson, R. Parrish, M. Horstwood, J. Fraser, and A. Tindle (2002), Textural, chemical and isotopic insights into the nature and behaviour of metamorphic monazite, *Chem. Geol.*, *191*, 183–207.

Furlong, K. P., and D. S. Chapman (2013), Heat flow, heat generation, and the thermal state of the lithosphere, *Annu. Rev. Earth Planet. Sci.*, *41*, 385–410.

GAF-BGR (2008), Final report: Réalisation des travaux de cartographie géologique de Madagascar, révision approfondie de la cartographie géologique et minière aux échelles 1/100 000 et 1/500 000 zone Sud. République de Madagascar, Ministère de l'Energie et des Mines EM/SG/DG/UCP/PGRM, *Geochim. Cosmochim. Acta*, *74*(5), 1579–1592.

Giese, J., A. Berger, G. Schreurs, and E. Gnos (2011), The timing of the tectono-metamorphic evolution at the Neoproterozoic-Phanerozoic boundary in central southern Madagascar, *Precambrian Res.*, *185*(3), 131–148.

Hacker, B. R., E. Gnos, L. Ratschbacher, M. Grove, M. McWilliams, S. V. Sobolev, J. Wan, and W. Zhenhan (2000), Hot and dry deep crustal xenoliths from Tibet, *Science*, *287*(5462), 2463.

Hacker, B. R., P. B. Kelemen, and M. D. Behn (2011), Differentiation of the continental crust by relamination, *Earth Planet. Sci. Lett.*, *307*(3), 501–516.

Hacker, B. R., P. B. Kelemen, and M. D. Behn (2015), Continental lower crust, *Annu. Rev. Earth Planet. Sci.*, *43*(1), 167–205.

Handke, M. J. (2001), Neoproterozoic magmatism in the Itremo region, central Madagascar: Geochronology, geochemistry, and petrogenesis, PhD thesis, Department of Earth and Planet. Sci., Washington Univ.

Handke, M. J., R. D. Tucker, and L. D. Ashwal (1999), Neoproterozoic continental arc magmatism in west-central Madagascar, *Geology*, *27*(4), 351–354.

Harley, S. L. (2008), Refining the P–T records of UHT crustal metamorphism, *J. Metamorph. Geol.*, *26*(2), 125–154.

Hetzel, R., I. Dunkl, V. Haider, M. Strobl, H. von Eynatten, L. Ding, and D. Frei (2011), Peneplain formation in southern Tibet predates the India-Asia collision and plateau uplift, *Geology*, *39*(10), 983–986.

Hinojosa, J. H., and K. L. Mickus (2002), Thermoelastic modeling of lithospheric uplift: a finite-difference numerical solution, *Comput. Geosci.*, *28*(2), 155–167.

Hofmeister, A. M., M. Pertermann, J. M. Branlund, and A. G. Whittington (2006), Geophysical implications of reduction in thermal conductivity due to hydration, *Geophys. Res. Lett.*, *33*, L11310, doi:10.1029/2006GL026036.

Hu, S., L. He, and J. Wang (2000), Heat flow in the continental area of China: A new data set, *Earth Planet. Sci. Lett.*, *179*, 407–419.

Ichiki, T., M. Ishikawa, J.-I. Kimura, R. Senda, and R. Rakotondrazafy (2015), Crustal assembly of the Antananarivo and Masora domains, central–eastern Madagascar: Constraints from U–Pb zircon geochronology and whole–rock geochemistry of meta–granitoids, *J. Mineral. Petrol. Sci. J-STAGE Adv. Publ.*, doi:10.2465/jmps.141225.

Jamieson, R. A., C. Beaumont, S. Medvedev, and M. H. Nguyen (2004), Crustal channel flows: 2. Numerical models with implications for metamorphism in the Himalayan-Tibetan orogen, *J. Geophys. Res.*, *109*, B06407, doi:10.1029/2003JB002811.

Jamieson, R. A., C. Beaumont, M. H. Nguyen, and D. Grujic (2006), Provenance of the Greater Himalayan sequence and associated rocks: Predictions of channel flow models, *Geol. Soc. London Spec. Publ.*, *268*(1), 165–182.

Jaupart, C., and J. C. Mareschal (2003), Constraints on crustal heat production from heat flow data, in *Treatise on Geochemistry, The Crust*, edited by R. L. Rudnick, Permagon, New York.

Jöns, N., and V. Schenk (2008), Relics of the Mozambique Ocean in the central East African Orogen: Evidence from the Vohibory block of southern Madagascar, *J. Metamorph. Geol.*, *26*(1), 17–28.

Jöns, N., and V. Schenk (2011), The ultrahigh temperature granulites of southern Madagascar in a polymetamorphic context: Implications for the amalgamation of the Gondwana supercontinent, *Eur. J. Mineral.*, *23*(2), 127.

Kelsey, D. E. (2008), On ultrahigh-temperature crustal metamorphism, *Gondwana Res.*, *13*(1), 1–29.

Kelsey, D. E., and M. Hand (2014), On ultrahigh temperature crustal metamorphism: Phase equilibria, trace element thermometry, bulk composition, heat sources, timescales and tectonic settings, *Geosci. Front.*, *6*(3), 311–356.

Kincaid, C., and P. Silver (1996), The role of viscous dissipation in the orogenic process, *Earth Planet. Sci. Lett.*, *142*(3), 271–288.

Kröner, A., I. Braun, and P. Jaeckel (1996), Zircon geochronology of anatectic melts and residues from a highgrade pelitic assemblage at Ihosy, southern Madagascar: Evidence for Pan-African granulite metamorphism, *Geol. Mag.*, *133*, 311–323.

Kröner, A., B. F. Windley, P. Jaeckelt, T. S. Brewer, and T. Razakamanana (1999), New zircon ages and regional significance for the evolution of the Pan-African orogen in Madagascar, *J. Geol. Soc.*, *156*(6), 1125–1135.

Lal, D., N. B. Harris, K. K. Sharma, Z. Gu, L. Ding, T. Liu, W. Dong, M. W. Caffee, and A. J. T. Jull (2004), Erosion history of the Tibetan Plateau since the last interglacial: Constraints from the first studies of cosmogenic ^{10}Be from Tibetan bedrock, *Earth Planet. Sci. Lett.*, *217*(1), 33–42.

Le Pichon, X., P. Henry, and B. Goffé (1997), Uplift of Tibet: From eclogites to granulites—Implications for the Andean Plateau and the Variscan belt, *Tectonophysics*, *273*(1), 57–76.

Lexa, O., K. Schulmann, V. Janoušek, P. Štípská, A. Guy, and M. Racek (2011), Heat sources and trigger mechanisms of exhumation of HP granulites in Variscan orogenic root, *J. Metamorph. Geol.*, *29*(1), 79–102.

Liang, S., W. Gan, C. Shen, G. Xiao, J. Liu, W. Chen, X. Ding, and D. Zhou (2013), Three-dimensional velocity field of present-day crustal motion of the Tibetan Plateau derived from GPS measurements, *J. Geophys. Res. Solid Earth*, *118*, 5722–5732, doi:10.1002/2013JB010503.

Lyubetskaya, T., and J. J. Ague (2009), Effect of metamorphic reactions on thermal evolution in collisional orogens, *J. Metamorph. Geol.*, *27*(8), 579–600.

Mareschal, J.-C., and C. Jaupart (2013), Radiogenic heat production, thermal regime and evolution of continental crust, *Tectonophysics*, *609*, 524–534.

Markl, G., J. Bäuerle, and D. Grujic (2000), Metamorphic evolution of Pan-African granulite facies metapelites from Southern Madagascar, *Precambrian Res.*, *102*(1), 47–68.

Martelat, J., C. Nicollet, J. Lardeaux, G. Vidal, and R. Rakotondrazafy (1997), Lithospheric tectonic structures developed under high-grade metamorphism in the southern part of Madagascar, *Geod. Acta*, *10*(3), 94–114.

Martelat, J.-E., J.-M. Lardeaux, C. Nicollet, and R. Rakotondrazafy (2000), Strain pattern and late Precambrian deformation history in southern Madagascar, *Precambrian Res.*, *102*(1), 1–20.

Martin, R. F., A. Randrianandraisana, and P. Boulvais (2013), Ampandrandava and similar phlogopite deposits in southern Madagascar formed from a silicocarbonatitic melt of crustal origin, *J. Afr. Earth Sci.*, *94*, 111–118.

McKenzie, D., and K. Priestley (2008), The influence of lithospheric thickness variations on continental evolution, *Lithos*, *102*(1), 1–11.

McLaren, S., and R. Powell (2014), Magmatism, orogeny and the origin of high-heat-producing granites in Australian Proterozoic terranes, *J. Geol. Soc.*, *171*(2), 149–152.

McLaren, S., M. Sandiford, and M. Hand (1999), High radiogenic heat-producing granites and metamorphism—An example from the western Mount Isa inlier, Australia, *Geology*, *27*(8), 679–682.

McLennan, S. M., W. B. Nance, and S. R. Taylor (1980), Rare earth element-thorium correlations in sedimentary rocks, and the composition of the continental crust, *Geochim. Cosmochim. Acta*, *44*(11), 1833–1839.

Mechie, J., S. V. Sobolev, L. Ratschbacher, A. Y. Babeyko, G. Bock, A. G. Jones, K. D. Nelson, K. D. Solon, L. D. Brown, and W. Zhao (2004), Precise temperature estimation in the Tibetan crust from seismic detection of the α-β quartz transition, *Geology*, *32*, 601–604.

Moine, B., V. Bosse, J.-L. Paquette, and E. Ortega (2014), The occurrence of a Tonian–Cryogenian (850 Ma) regional metamorphic event in Central Madagascar and the geodynamic setting of the Imorona–Itsindro (800 Ma) magmatic suite, *J. Afr. Earth Sci.*, *94*, 58–73.

Muller, B. G. J. (2000), The evolution and significance of the Bongolava-Ranotsara shear zone Madagascar [Thesis], Rand Afrikaans Univ., Johannesburg, South Africa, 125 pp.

Nabelek, P. I., A. G. Whittington, and A. M. Hofmeister (2010), Strain heating as a mechanism for partial melting and ultrahigh temperature metamorphism in convergent orogens: Implications of temperature-dependent thermal diffusivity and rheology, *J. Geophys. Res.*, *115*, B12417, doi:10.1029/2010JB007727.

Nédélec, A., E. W. Stephens, and A. E. Fallick (1995), The Panafrican stratoid granites of Madagascar: Alkaline magmatism in a post-collisional extensional setting, *J. Petrol.*, *36*(5), 1367–1391.

Nicollet, C. (1989), L'eclogite de Faratsiho (Madagascar): Un cas exceptionnel de métamorphisme de haute-P-basse-T au Protérozoïque supérieur, *Precambrian Res.*, *45*(4), 343–352.

Nicollet, C. (1990), Crustal evolution of the granulites of Madagascar, *Granulites Crustal Evol.*, *31*, 291–310.

Paquette, J. L., and A. Nédélec (1998), A new insight into Pan-African tectonics in the East–West Gondwana collision zone by U-Pb zircon dating of granites from central Madagascar, *Earth Planet. Sci. Lett.*, *155*(1–2), 45–56.

Paquette, J. L., A. Nédélec, B. Moine, and M. Rakotondrazafy (1994), U-Pb, single zircon Pb-evaporation, and Sm-Nd isotopic study of a granulite domain in SE Madagascar, *J. Geol.*, *102*, 523–538.

Partin, C. A., et al. (2013), Large-scale fluctuations in Precambrian atmospheric and oceanic oxygen levels from the record of U in shales, *Earth Planet. Sci. Lett.*, *369*, 284–293.

Rakotondrazafy, R., S. Pierdzig, M. M. Raith, and S. Hoernes (1997), Phlogopite-Mineralisations in the Beraketa belt of southern Madagascar: A spectacular example of channelised fluid flow and fluid-rock interaction, *Gondwana Res. Group Misc. Publ.*, *5*, 81–82.

Rapp, R. P., and E. B. Watson (1986), Monazite solubility and dissolution kinetics: Implications for the thorium and light rare earth chemistry of felsic magmas, *Contrib. Mineral. Petrol.*, *94*(3), 304–316.

Rapp, R. P., F. J. Ryerson, and C. F. Miller (1987), Experimental evidence bearing on the stability of monazite during crustal anatexis, *Geophys. Res. Lett.*, *14*(3), 307–310, doi:10.1029/GL014i003p00307.

Ray, L., H.-J. Förster, A. Förster, S. Fuchs, R. Naumann, and O. Appelt (2015), Tracking the thermal properties of the lower continental crust: Measured versus calculated thermal conductivity of high-grade metamorphic rocks (Southern Granulite Province, India), *Geothermics*, *55*, 138–149.

Reid, M. R., S. R. Hart, E. R. Padovani, and G. A. Wandless (1989), Contribution of metapelitic sediments to the composition, heat production, and seismic velocity of the lower crust of southern New Mexico, USA, *Earth Planet. Sci. Lett.*, *95*, 367–381.

Rubatto, D., S. Chakraborty, and S. Dasgupta (2013), Timescales of crustal melting in the Higher Himalayan Crystallines (Sikkim, Eastern Himalaya) inferred from trace element-constrained monazite and zircon chronology, *Contrib. Mineral. Petrol.*, *165*, 349–372.

Rudnick, R. L., and S. Gao (2003), Composition of the continental crust, *Treatise on Geochemistry*, *3*, 1–64.

Rudnick, R. L., and S. Gao (2014), Composition of the continental crust, *Treatise Geochem.*, *3*, 1–51.

Rudnick, R. L., and I. Jackson (1995), Measured and calculated elastic wave speeds in partially equilibrated mafic granulite xenoliths: Implications for the properties of an underplated lower continental crust, *J. Geophys. Res.*, *100*(B6), 10,211–10,218, doi:10.1029/94JB03261.

Rudnick, R. L., and T. Presper (1990), Geochemistry of intermediate/-to high-pressure granulites, in *Granulites and Crustal Evolution*, pp. 523–550, Springer, New York.

Sandiford, M., and S. McLaren (2002), Tectonic feedback and the ordering of heat producing elements within the continental lithosphere, *Earth Planet. Sci. Lett.*, *204*(1–2), 133–150.

Schreurs, G., J. Giese, A. Berger, and E. Gnos (2010), A new perspective on the significance of the Ranotsara shear zone in Madagascar, *Int. J. Earth Sci.*, *99*(8), 1827–1847.

Shi, D., Z. Wu, S. L. Klemperer, W. Zhao, G. Xue, and H. Su (2015), Receiver function imaging of crustal suture, steep subduction, and mantle wedge in the eastern India–Tibet continental collision zone, *Earth Planet. Sci. Lett.*, *414*, 6–15.

Sizova, E., T. Gerya, and M. Brown (2014), Contrasting styles of Phanerozoic and Precambrian continental collision, *Gondwana Res.*, *25*, 522–545.

Stearns, M. A., B. R. Hacker, L. Ratschbacher, J. Lee, J. M. Cottle, and A. Kylander-Clark (2013), Synchronous Oligocene–Miocene metamorphism of the Pamir and the north Himalaya driven by plate-scale dynamics, *Geology*, *41*, 1071–1074.

Stern, R. J. (1994), Arc-assembly and continental collision in the Neoproterozoic African orogen: Implications for the consolidation of Gondwanaland, *Annu. Rev. Earth Planet. Sci.*, *22*, 319–351.

Stüwe, K. (1998), Heat sources of Cretaceous metamorphism in the Eastern Alps—A discussion, *Tectonophysics*, *287*(1), 251–269.

Stüwe, K. (2007), *Geodynamics of the Lithosphere: An Introduction*, 493 pp., Springer, New York.

Taylor, R. J., C. Clark, I. C. Fitzsimons, M. Santosh, M. Hand, N. Evans, and B. McDonald (2014), Post-peak, fluid-mediated modification of granulite facies zircon and monazite in the Trivandrum Block, southern India, *Contrib. Mineral. Petrol.*, *168*(2), 1–17.

Taylor-Jones, K., and R. Powell (2015), Interpreting zirconium-in-rutile thermometric results, *J. Metamorph. Geol.*, *33*, 115–122.

Thomas, J. B., E. B. Watson, F. S. Spear, P. T. Shemella, S. K. Nayak, and A. Lanzirotti (2010), TitaniQ under pressure: the effect of pressure and temperature on the solubility of Ti in quartz, *Contrib. Mineral. Petrol.*, *160*(5), 743–759.

Thompson, A. B., and J. A. Connolly (1995), Melting of the continental crust: Some thermal and petrological constraints on anatexis in continental collision zones and other tectonic settings, *J. Geophys. Res.*, *100*(B8), 15,565–15,579, doi:10.1029/95JB00191.

Tucker, R., J. Roig, P. Macey, C. Delor, Y. Amelin, R. Armstrong, M. Rabarimanana, and A. Ralison (2011), A new geological framework for south-central Madagascar, and its relevance to the "out-of-Africa" hypothesis, *Precambrian Res.*, *185*(3), 109–130.

Tucker, R. D., T. M. Kusky, R. Buchwaldt, and M. J. Handke (2007), Neoproterozoic nappes and superposed folding of the Itremo Group, west-central Madagascar, *Gondwana Res.*, *12*(4), 356–379.

Tucker, R. D., J. Y. Roig, B. Moine, C. Delor, and S. G. Peters (2014), A geological synthesis of the Precambrian shield in Madagascar, *J. Afr. Earth Sci.*, *94*, 9–30.

Unsworth, M. J., et al. (2005), Crustal rheology of the Himalaya and Southern Tibet inferred from magnetotelluric data, *Nature*, *438*(7064), 78–81.

Watt, G. R., and S. L. Harley (1993), Accessory phase controls on the geochemistry of crustal melts and restites produced during water-undersaturated partial melting, *Contrib. Mineral. Petrol.*, *114*(4), 550–566.

Whitehouse, M. J., G. R. R. Kumar, and A. Rimša (2014), Behaviour of radiogenic Pb in zircon during ultrahigh-temperature metamorphism: An ion imaging and ion tomography case study from the Kerala Khondalite Belt, southern India, *Contrib. Mineral. Petrol.*, *168*, 1–18.
Whittington, A. G., A. M. Hofmeister, and P. I. Nabelek (2009), Temperature-dependent thermal diffusivity of the Earth's crust and implications for magmatism, *Nature*, *458*(7236), 319–321.
Windley, B. F., A. Razafiniparany, T. Razakamanana, and D. Ackermand (1994), Tectonic framework of the Precambrian of Madagascar and its Gondwana connections: A review and reappraisal, *Geol. Rundsch.*, *83*(3), 642–659.
Wolf, M. B., and D. London (1995), Incongruent dissolution of REE-and Sr-rich apatite in peraluminous granitic liquids: Differential apatite, monazite, and xenotime solubilities during anatexis, *Am. Mineral.*, *80*(7), 765–775.
Zhu, X. K., and R. K. O'nions (1999), Zonation of monazite in metamorphic rocks and its implications for high temperature thermochronology: A case study from the Lewisian terrain, *Earth Planet. Sci. Lett.*, *171*, 209–220.